Report on calibration campaigns for pyrheliometer and pyranometer

SFERA II Project	
Solar Facilities for the European Research Area - Second Phase	
Grant agreement number:	312643
Start date of project:	01/01/2014
Duration of project:	48 months
WP11 – Task 1.X	Deliverable 11.3
Due date:	12/2016
Submitted	12/2016
File name:	SFERA2PyrhelCal_D11_3
Partner responsible	DLR
Person responsible	Bijan Nouri
Author(s):	Bijan Nouri, Stefan Wilbert, Ginés García, Lourdes Ramírez, Luis Zarzalejo, Rita Valenzuela, Francisco Ferrera, Emmanuel Guillot
Dissemination Level	Public

List of content

Abstract 3
1 Introduction 4
2 Update on calibration facility 5
2.1 Introduced innovations on calibration facility 6
2.2 Used references devices 6
3 Calibration execution and evaluation method 7
3.1 Comments on ACR operation 7
3.2 Treatment of ACR data 8
4 Description of the individual campaigns 10
4.1 Ambient conditions of calibration campaigns 10
4.2 Results of the pyrheliometer calibration 14
4.2.1 Obtained valid data 14
4.2.2 Discussion of pyrheliometer calibration results 18
4.3 Results of the pyranometer calibrations with continuous sun-and-shade method 22
4.3.1 Obtained valid DNI and DHI reference 22
4.3.2 Discussion of Pyranometer results continuous sun-and-shade method 26
4.3.2.1 Solar zenith and azimuth angle dependency of pyranometer responsivity 30
4.3.2.2 Detailed discussion of historical sensor responsivity evolution for some sensors 33
4.4 Results Pyranometer calibration alternating sun-and-shade method 38
4.4.1 Obtained valid DNI, DHI and GHI data from reference and test device 38
4.4.2 Discussion of results for the alternating sun-and-shade method 41
4.5 Influence of cloud filtering on sensor responsivity – filtering with a whole sky imager system 42
5 Conclusion 44

Abstract

Accurate measurements of solar irradiance are crucial for the planning, tests and operation of solar power plants. The measurement uncertainty caused by the calibration is the most relevant contribution to the overall uncertainty of well-maintained radiometers. Uncertainties of field pyranometers and pyrheliometers can be significantly reduced by calibrations through WRR (World Radiometric Reference) traceable reference sensors compared to indoor calibrations.
The following tasks were carried out:

- Improvements of the existing PSA (Plataforma Solar de Almeria) calibration facility for pyrheliometer and pyranometer
- Conducting and evaluating three calibration campaigns according to the ISO standards 9059 [ISO, 1990] and 9846 [ISO, 1993]
    - First campaign period 19.06.2014 to 30.06.2014
    - Second campaign period 23.09.2015 to 09.10.2015
    - Third campaign period 20.06.2016 to 30.06.2016
- A two week stay of a CNRS scientist during the 2016 calibration campaign at the PSA

This report presents the results of the three campaigns, in which new responsivities were derived for 80 field sensors. The presentation of the results includes:

- Comparison of newly acquired responsivities with manufacturer responsivity
- Comparison of repeatedly calibrated sensors at PSA during varies calibration campaigns
- Solar angle dependency of pyranometers
- Reliability of manufacturer responsivities
- Influence of an automated cloud filtering system on basis of whole sky imagers (cloud cameras)

1 Introduction

Pyrheliometer and pyranometer devices are used to measure the solar irradiance. Where pyrheliometers have to be tracked towards the sun in order to measure the direct normal irradiance (DNI), pyranometers can be mounted horizontally to measure the global horizontal irradiance (GHI). When the direct sunlight from the sun is blocked via a shading object, pyranometers can be used to measure the diffuse horizontal irradiance (DHI).

The calibration uncertainty is the most relevant contribution of the overall measurement uncertainty of these devices if they are used according to best practices guidelines. Generally all calibration methods compare the voltage raw signal of the test device with the irradiance signal of a reference device. For pyranometers, the reference signal can also be a calculated reference GHI value from a reference DNI and DHI signal. This is the preferable procedure since the DNI can be measured with a highly accurate absolute cavity radiometer (ACR), so that the calculate GHI can be actually more accurate than a directly measured GHI. In any case the reference device should be traceable to the world radiometric reference (WRR) in Davos. The main differences between existing calibration methods are typically the data preprocessing and filtering.

At the joint calibration facility at PSA (Plataforma Solar de Almeria) pyrheliometers are calibrated according to the standard ISO 9059 using two ACRs as reference. Pyranometers are calibrated according to the continuous sun-and-shade method (CoSSM) and the alternating sun-and-shade method (ASSM). Both pyranometer calibration methods are described in the ISO standard 9846. For the CoSSM two ACRs and a CMP22 pyranometer operated as DHI sensor are used as reference. Compared with that the ASSM needs only the ACRs as reference and was used to calibrate the DHI reference CMP22 sensor. ASSM is only used for the reference pyranometer, since a parallel calibration of several sensors with the ASSM is only possible with the massive use of hardware and manual work.

2 Update on calibration facility

The work on the calibration test bench for pyrheliometer and pyranometer at the PSA METAS facility started in 2014. A first functional stage of development was reached in June 2014. Since then, the calibration facility was continuously optimized. A detail description of the facility, for the state up to October 2015, was delivered in the task report D11.2 [Sfera2 D11_2, 2015]. In this report only a short overview on the facility is given, mainly focused on the innovations introduced since October 2015. The main elements of the calibration facility are:

- Sensor test bench for pyranometer test sensors (see **Figure 1** (image top detail number one))
- Cloud camera monitoring sky conditions at calibration site
- Black Photon Tracker with CMP22 DHI reference Pyranometer (see **Figure 1** bottom left)
- Heliostat tracking system for test Pyrheliometers and absolute cavity reference radiometer (ACR) (see **Figure 1** bottom left centre and bottom right centre)
- Metas wind mast with ambient temperature, humidity, pressure, wind speed and wind direction measurements (see **Figure 1** bottom right)

Figure 1. **Top) Overview of Metas calibration setup (1: Pyranometer test bench; 2: Pyrheliometers test bench; 3: Black Photon tracker with DHI reference; 4: cloud camera); Bottom left) detail view of Black Photon tracker; Bottom left centre) detail view of pyrheliometer test bench; Bottom right centre) two absolute cavity reference pyrheliometers located at pyrheliometer test benchfront cabinet; Bottom right) Metas wind mast.**

2.1 Introduced innovations on calibration facility

New pyranometer test bench

Southeast of the pyrheliometers test bench, a rigid sensor test bench was erected (**Figure 1**), providing mounting space for up to 20 pyranometers. Each pyranometer is placed on a mounting plate at the end of a crossbeam. The mounting plate consists of a standard mane plate and a second adjustable sensor holder. This way various pyranometer models with and without ventilation unit can be installed, without adapting the standard structure. The new facility has been constructed as a copy of a Meteoswiss test bench at Payerne, thanks to the collaboration of its research staff.

At the western side of the sensor test bench an electrical cabinet is installed, which holds the electrical power supply and the data acquisition system (DAS) for the test pyranometers. The DAS consist of two Measuresoft IMP 35951C analogue reed relays which communicate directly via SNET with the pyrheliometer test bench control computer. Measured data are written into the already existing pyrheliometer test bench data file, thus an additional time synchronisation for the pyranometer data is not necessary. Due to the lack of the thermistor measurement capacities of the IMP devices, an additional Campbell Scientific CR1000 data logger for pyranometer with thermistors sensors for the internal sensor temperature were introduced.

New sun tracker for DHI reference

On top of the southern METAS container a sun tracker from the company Black Photon was erected (see **Figure 1**), holding the DHI reference. With the automatically controllable shade structure, the Black Photon sun tracker is suited for the alternating sun-and-shade pyranometer calibration method. An individual DAS system, consisting of a Campbell Scientific CR1000 data logger, collects all data from the instrumentation mounted on the sun tracker.

2.2 Used references devices

During the three performed calibration campaigns, different reference sensors were used. For the DNI always a redundant setup consisting of two PMO6-CC ACRs and for the DHI a single shaded CMP22 pyranometer (see Table 1).

Table 1. **At calibration campaigns used reference sensors**

	2014	2015	2016
DNI reference signal	PMO6-CC 0106 PMO6-CC 0807	PMO6-CC 0108 PMO6-CC 0807	PMO6-CC 0106 PMO6-CC 0807
DHI reference signal	CMP22 110288	CMP22 110288	CMP22 110288

3 Calibration execution and evaluation method

Three individual calibration campaigns were carried out.

- First campaign period 19.06.2014 to 30.06.2014
- Second campaign period 23.09.2015 to 09.10.2015
- Third campaign period 20.06.2016 to 30.06.2016

The campaigns were jointly operated by Ciemat and DLR personal, with extra support from CNRS during the third campaign.

All three campaigns include pyrheliometer calibration according to the ISO standard 9059 and pyranometer calibration according to the ISO standard 9846 continuous sun-and-shade method. Additionally, a pyranometer calibration according to the ISO standard 9846 alternating sun-and-shade method was carried out in 2015. Detailed descriptions of the used calibration execution procedure and evaluation methods are stated in the previous task report [Sfera2 D11_2, 2015].

3.1 Comments on ACR operation

During the three calibration campaigns some technical challenges, concerning the reference ACRs, occurred.

2014 calibration campaign

Over the entire calibration period an average deviation of 0.41% was observed (based on the signal of the device PMO6-CC 0106). The observed deviation was with a standard deviation of about 0.03% stable.

All ACRs were calibrated in the World Radiation Center (WRC) Davos compared to a reference ACR using the sun as source. The WRC reference ACR is periodically calibrated against the World Standard Group (WSG). Before the PSA calibration campaign neither of the participating ACRs had been tested at an international intercomparison, however in September of 2014 the DLR ACR PMO6-CC 0807 was participating at the NREL pyrheliometer comparison (NPC-2014). During the NPC-2014 a correction factor of 1.0045 was generated for the DLR ACR. Applied on the calibration data, the deviation between the ACRs was reduced from an average deviation from 0.41% to -0.035%. This remaining difference is considered negligible and could be explained due to the PMO6-CC 0106 had never been tested at an international comparison and a correction factor had not been applied. The cause for the deviation of the DLR device was an erroneous implemented factory calibration of the ACR.

Both ACRs are controlled via RS232 port from a control computer. A configuration order is send to the ACRs before each series. The objective is a parallel operation of both ACRs. Small fluctuations up to one second between the ACRs time stamps were observed. Since the time deviation fluctuates permanently between 0 and 1 second, it is assumed that this is triggered by rounding processes during the creation of the time stamps. The control computer is sending the order sequentially to the ACRs. In the case of time deviations, the timestamp of the ACR that receives the order first is always ahead of the other ACR timestamp.

High internal temperatures of the ACR control units around 20°C above the ambient temperature were observed. The acceptable ambient temperature of the ACR control units is estimated as 0°C to 40°C [PMOD, 2009]. At the calibration site ambient temperature at the upper limit of the range were reached, which lead to internal temperatures up to 60°C. According to the ACR manufacturer PMOD, internal temperatures below 70°C are desirable, while the specifications of the bulk of the ACR components actually show a range of -40°C to 85°C [PfiffnerEmail, 2016]. The ACR control unit takes the internal temperature into account, while evaluating the current measurement value.

2015 calibration campaign

For protection against environmental influences, both ACRs were placed inside an electrical cabinet in all three calibration campaigns. During the measurements two shutters of this cabinet were opened, giving the line of sight for the ACRs free. In 2015 one of the shutters did not open repeatedly, which lead to a partial loss of ACR measurements from one sensor. An exchange of a power supply to more potent device solved this problem.

2016 calibration campaign

At the beginning of the 2016 campaign not the device PMO6-CC 0106 as stated in Table 13 was implemented, but the more recently calibrated PMO6-CC 0301 was mounted. Due to a technical malfunction of this ACRs internal shutter, the replacement of the PMO6-CC 0301 was unavoidable.

In the same year two series of the device PMO6-CC 0807 were lost, due to communication problem between the control computer and the ACR control unit. Additional communication errors lead to a malfunction of the pyrheliometer test bench, which run into a physical limit switch. This resulted in a data loss on two late evenings.

The redundant implementation of the ACR sensors was essential for these calibration campaigns. Despite all technical challenges at least one sensor was always operable. For a predominant part of the calibration period redundant ACR data were available, which allowed an almost constant signal plausibility check in between both ACRs. The average deviation of the valid data between both ACRs applying the final ACR calibration constants was below 0.1% for all three campaigns (compared to the average value of both ACRs).

3.2 Treatment of ACR data

The DNI measurement process of the Pmod PMO6-CC ACRs consists of an open and a closed phase. Each phase last 60 seconds, but the actually measurement of each phase consists only of the last 10 seconds of each phase (stated interval durations can be adapted). During the open phase the sensor shutter is open and the thermal impedance is illuminated. The absorbed solar radiation flows through the impedance to a heat sink which leads to a measureable temperature difference across the impedance. During the closed phase an electrical heater substitutes the solar radiation energy until the same temperature difference across the impedance is reached. By the end of the closed phased the DNI value of the previous open phase is calculated [PMOD, 2009]. For the instruments under calibration and all other involved signals a temporal resolution of one second is used and, average values are generated corresponding to the last 10 seconds of each open phase.

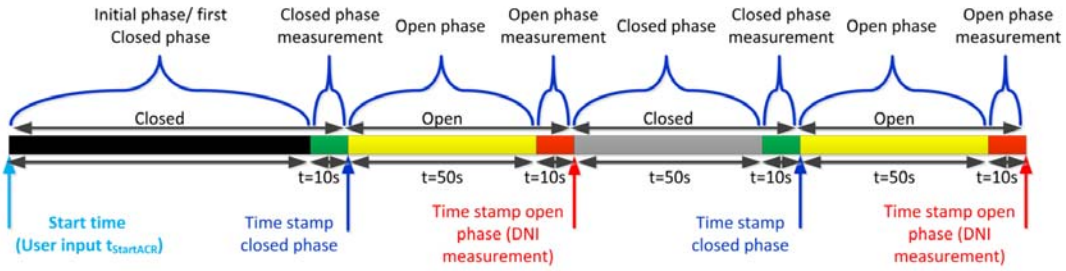

Figure 2. **Order of events absolute cavity DNI measurement (based on [PMOD, 2009])**

4 Description of the individual campaigns

All 28 measurement days during the three calibration campaign are listed in Table 2. After varies filtration processes 16 measurement days with valid data remained for the three calibration campaigns. The filtration process will be discussed in more detail in the chapters 4.2.1 and 4.3.1.

Table 2. **Entire list of carried out measurement days with comments of data status**

Date	Used for calibration	Day	Comment
06.06.2014	No		System trial, no usable data
13.06.2014	No		System trial, no usable data
16.06.2014	No		Cloudy conditions, no usable data
17.06.2014	No		Cloudy conditions, no usable data
18.06.2014	No		ACR signals not synchronized, no usable data
19.06.2014	Yes	1	High turbidity, short valid time window around solar noon
20.06.2014	Yes	2	High turbidity, valid time window around solar noon
25.06.2014	Yes	3	Cloudy conditions with short clear moments
26.06.2014	Yes	4	Valid data in the morning, clouds in the afternoon
27.06.2014	Yes	5	Clear sky day with partially invalid data due to strong wind
30.06.2014	Yes	6	Clear sky day with only short valid time window due to strong wind
23.09.2015	Yes	1	Cloudy conditions with short clear moments
24.09.2015	No	2	Cloudy conditions with short clear moments, no usable data
25.09.2015	Yes	3	Clear sky day with partially invalid data due to some scattered clouds
28.09.2015	No	4	Cloudy conditions, no usable data
30.09.2015	No	5	Cloudy conditions, no usable data
01.10.2015	Yes	6	Light mist in the morning, afterwards clear sky conditions, some cloud influence at the late afternoon
02.10.2015	Yes	7	Clear sky day with partially invalid data due to some scattered clouds
06.10.2015	No	8	General clear conditions with constant scattered clouds, no usable data
09.10.2015	No	9	General clear conditions with constant scattered clouds, no usable data
20.06.2016	Yes	1	Clear sky day with partially invalid data due to some scattered clouds
21.06.2016	Yes	2	Clear sky day with partially invalid data due to strong wind
22.06.2016	Yes	3	Clear sky day with partially invalid data due to strong wind
23.06.2016	Yes	4	Clear sky day with partially invalid data due to strong wind
24.06.2016	Yes	5	Clear sky day with partially invalid data due to some scattered clouds
27.06.2016	No	6	Clear sky day with no valid data due to strong wind and some scattered clouds
29.06.2016	Yes	7	Clear sky day with partially invalid data due to strong wind
30.06.2016	No	8	Clear sky day, no data due to malfunction of DAS

4.1 Ambient conditions of calibration campaigns

The **Figure 3**, **Figure 4** and **Figure 5** illustrate the occurred ambient conditions during the three calibration campaigns. Time stamps correspond to already preselected ACR data, but not yet finally filtered for the evaluation of the calibration. The further filtering process will be presented in chapter 4.2 and 4.3.

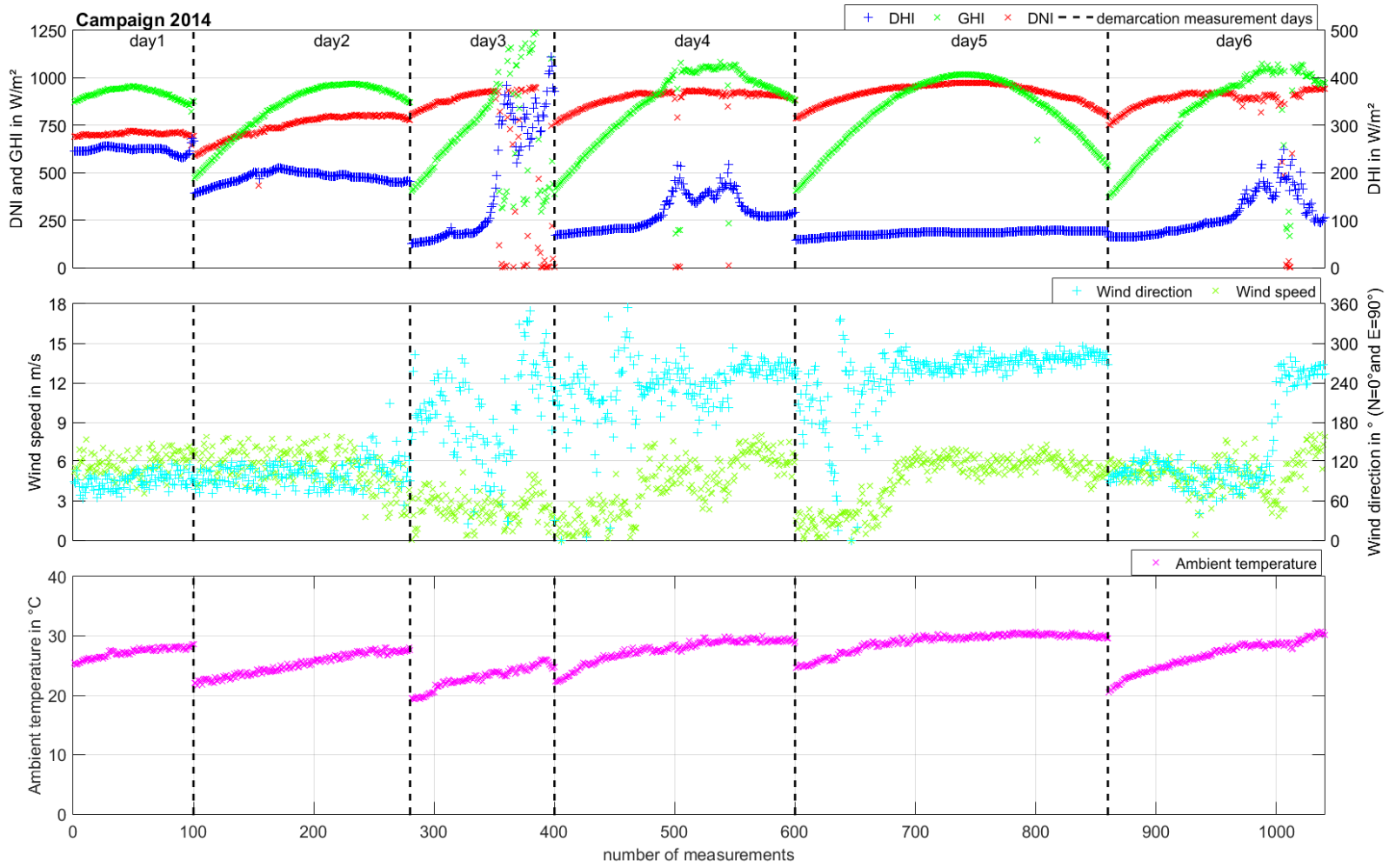

Figure 3. **Ambient conditions during 2014 calibration campaign (day 1: 19.06.2014, day 2: 20.06.2014, day 3: 25.06.2014, day 4: 26.06.2014, day5: 27.06.2014 and day 6: 30.06.2014)**

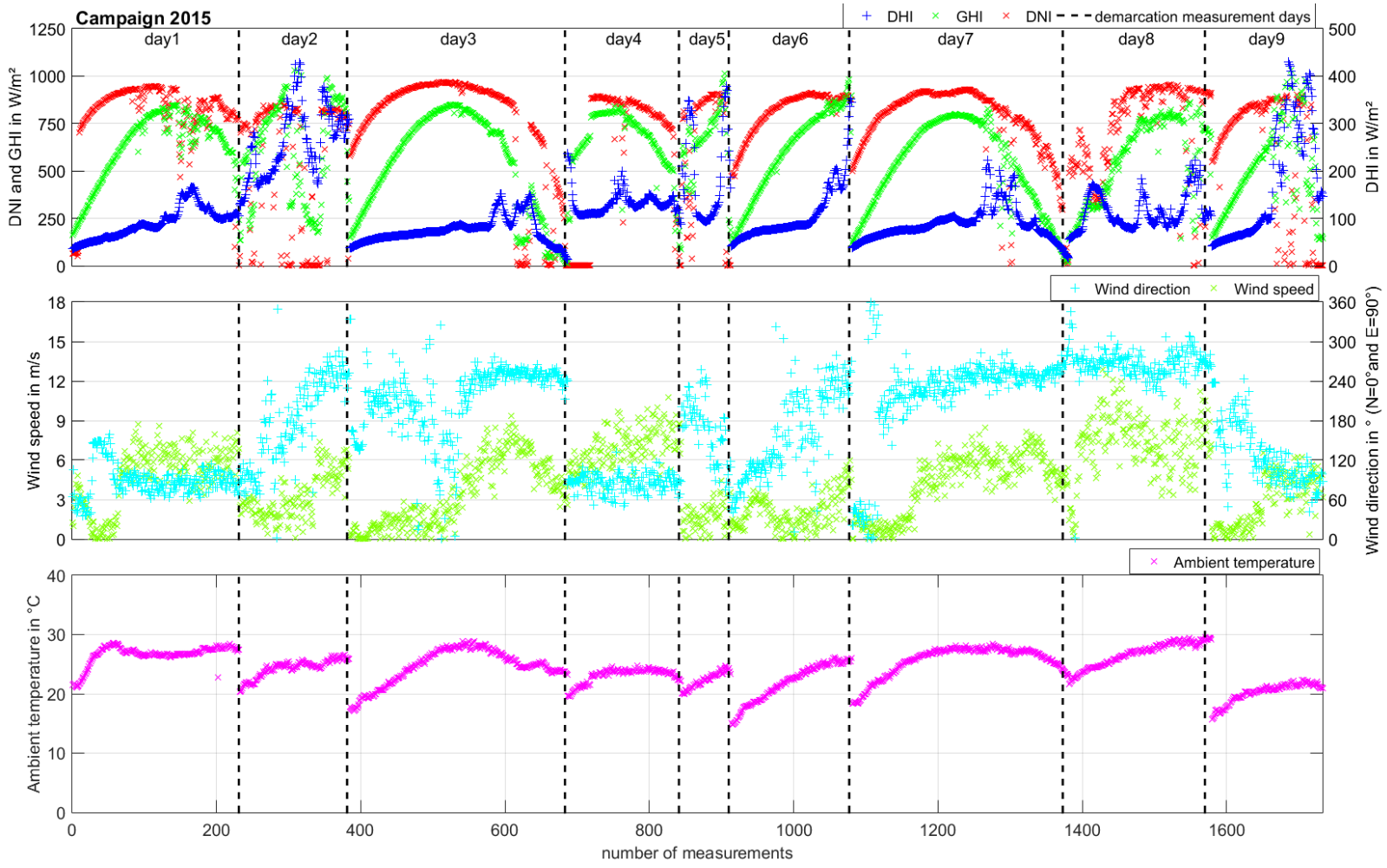

Figure 4. **Ambient conditions during 2015 calibration campaign (day 1: 23.09.2015, day 2: 24.09.2015, day 3: 25.09.2015, day 4: 28.09.2015, day5: 30.09.2015, day 6: 01.10.2015, day 7: 02.10.2015, day 8: 06.10.2015 and day 9: 09.10.2015)**

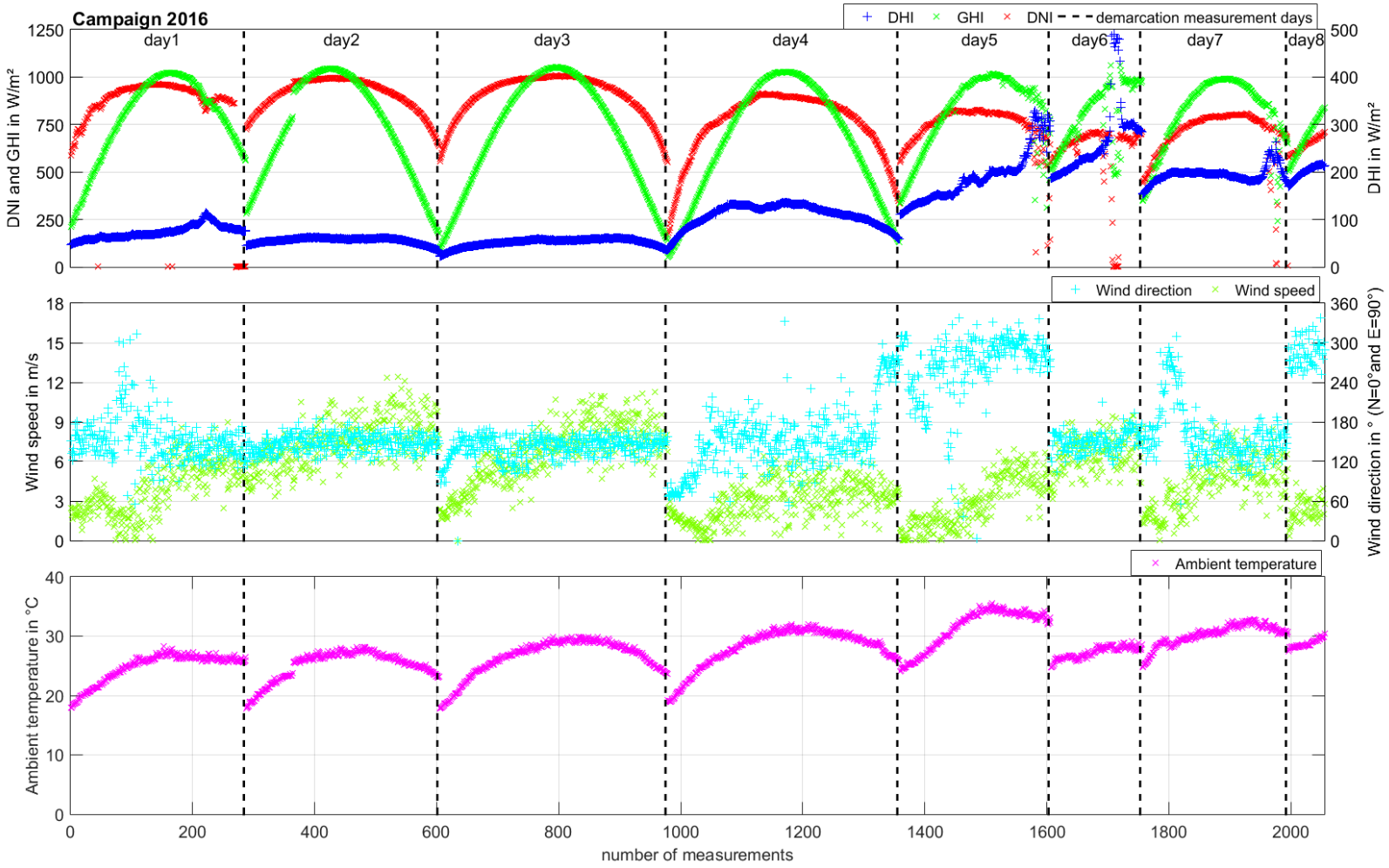

Figure 5. **Ambient conditions during 2016 calibration campaign (day 1: 20.06.2016, day 2: 21.06.2016, day 3: 22.06.2016, day 4: 23.06.2016, day5: 24.06.2016, day 6: 27.06.2016, day 7: 29.06.2016 and day 8: 30.06.2016)**

4.2 Results of the pyrheliometer calibration

4.2.1 Obtained valid data

After the data pre-processing, the pre-processed data are filtered according to the ISO standard 9059. Series of a time-period of 40 minutes (corresponding with each ACR series) has been defined. Two minutes are needed for a 10 seconds integrated measurement from ACR devices. Thus, each series can have 20 pairs of 10 seconds integrated values (points) for the calibration of each sensor. The following filters were active (in this order):

- DNI<700 W/m²
- Linke turbidity < 6
- Wind from sun azimuth ±30° with wind speed larger 5 m/s
- Due to influence of clouds (based on METAS cloud camera)
    - Cloud cover ≤ 12.5%
    - Angular distance to sun ≥15°
- Series with less than 10 valid measurement values (points)
- Series with F(i,j) values which deviate by more than ±2% from corresponding F(j) value

Figure 6, Figure 7 and Figure 8 illustrate the DNI reference signal and the filters causing the data rejection. They also list the share of the individual filters. For 2014 and 2016 around 50% of the initial data is considered as valid. Due to bad wetter conditions with a strong influence from many scattered clouds less than 16% of the initial data are considered as valid for the 2015 calibration.

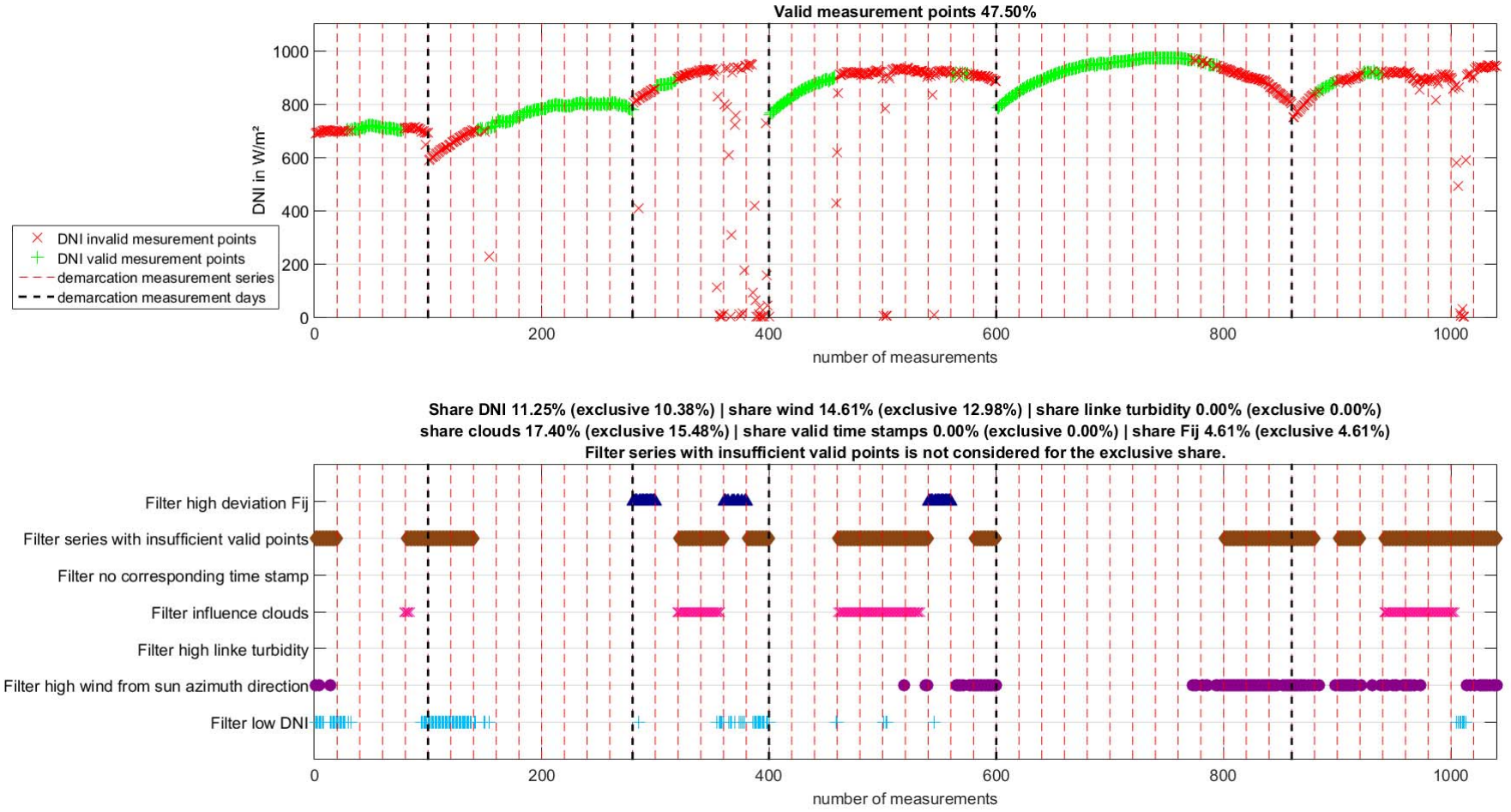

Figure 6. **2014 pyrheliometer campaign; Top) valid and invalid reference data; Bottom) marker for active filter of the invalid data**

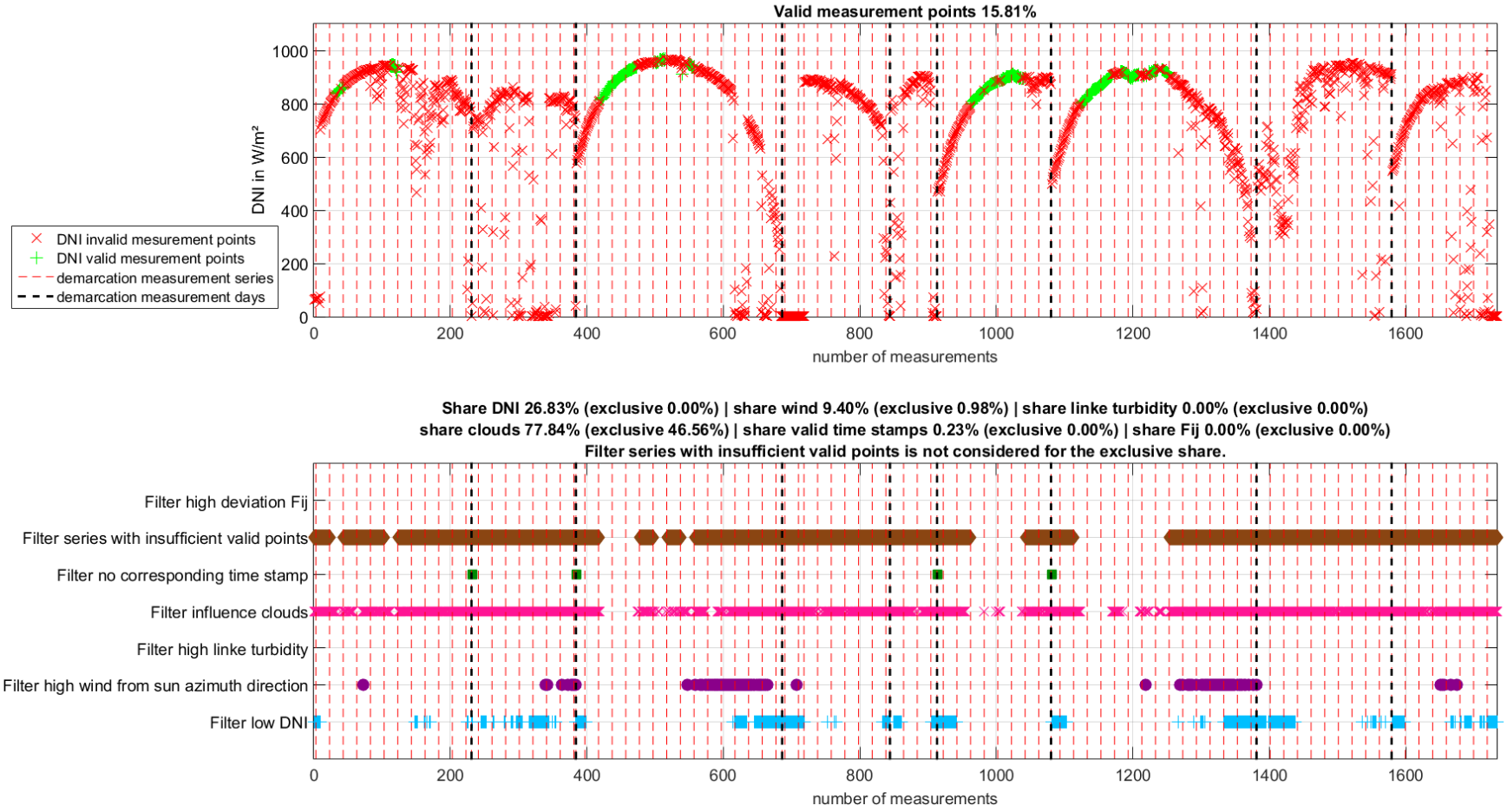

Figure 7. **2015 pyrheliometer campaign; Top) valid and invalid reference data; Bottom) marker for active filter of the invalid data**

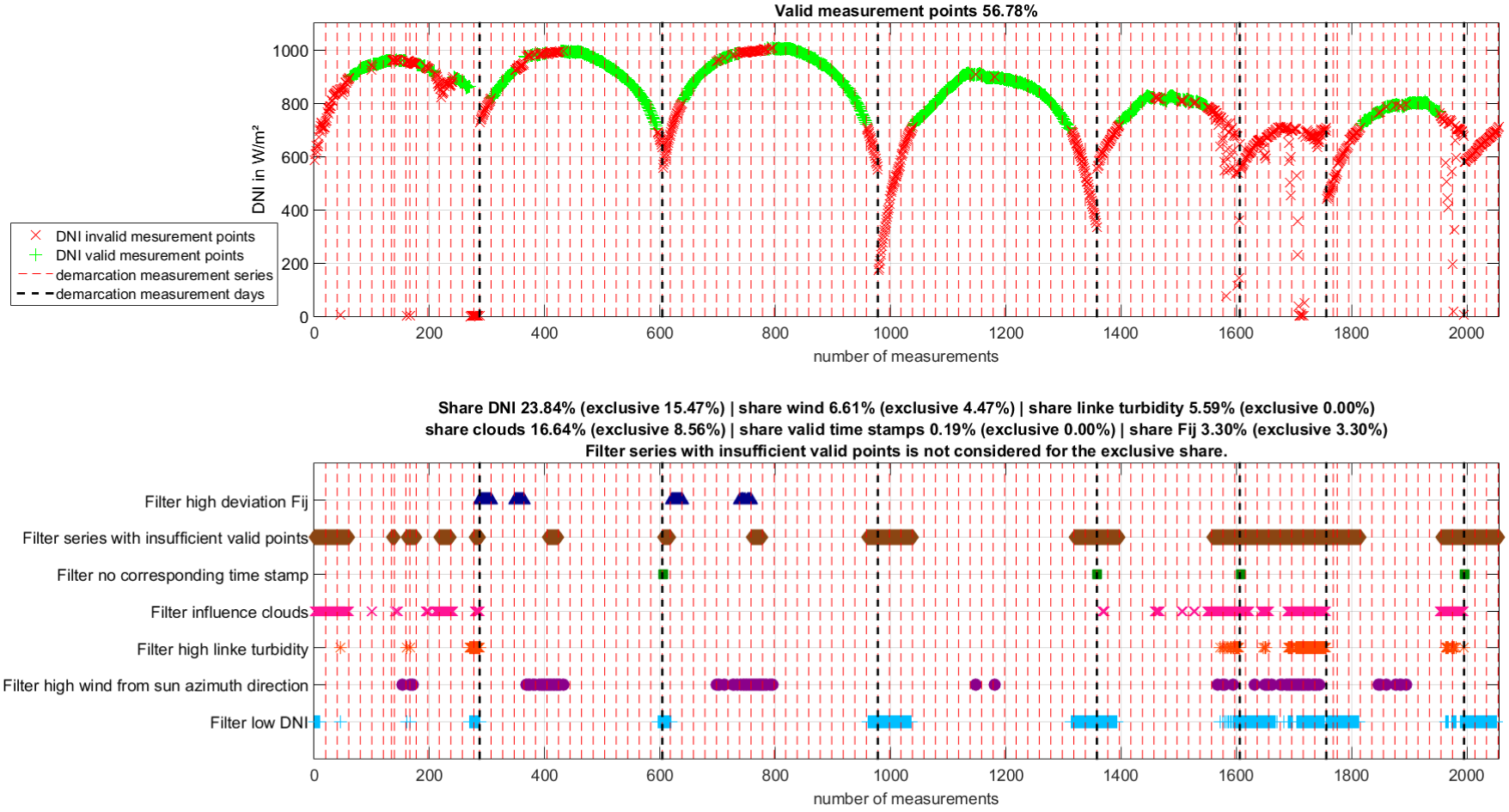

Figure 8. **2016 pyrheliometer campaign; Top) valid and invalid reference data; Bottom) marker for active filter of the invalid data**

4.2.2 Discussion of pyrheliometer calibration results

Over the three campaigns a total of 51 new responsivities distributed over 39 individual field pyrheliometers were derived from the measurement data. In most of the cases only small deviations below 1%/year between the new responsivities and the responsivity from the previous calibration were found. Table 3 list all field pyrheliometers, which were participating at the PSA calibration campaigns. Some sensors were repeatedly in varies campaigns calibrated. Additionally to the new and old responsivity are also the standard deviation (std) and relative standard deviation (rsd) stated. The Std and rsd are calculated via the responsivity values for each series (R_j).

Equation 1

$$rsd = \frac{std}{\bar{x}} \cdot 100 = \sqrt{\frac{1}{n-1}\sum_{i=1}^{n}(x_i - \bar{x})^2} \Big/ \bar{x} \cdot 100$$

For the three sensors CHP1_060495, Nip_20119E6 and Nip_18949E6 the newly derived responsivity showed large deviations >3% to the previous responsivity (see Table 3). No technical defects were detected and since the operation and calibration history of these sensors is not well documented, a cause could not be found. The NIPs were not calibrated for many years so that the change of the calibration constant actually lies below 1%/year. From these three sensors, only the device Nip_20119E6 was repeatedly calibrated at the PSA (in all three campaigns). Within the PSA calibrations, no significant deviations were observed. Due to a cable malfunction for the sensor CH1_010270 repeated data losses occurred, which lead to a shorter data base. For the further statistics these sensors were considered as outliers and are therefore excluded.

Table 3. **List on calibration campaigns participating field pyrheliometer with results for new responsivity**

year	Model	Serial number	Comment	New responsivity in µV/(W/m²)	Std of responsivity (Rj) in µV/(W/m²)	Rsd of new responsivity in %	Old responsivity in µV/(W/m²)	Deviation to most recent older responsivity in %
14	K&Z CHP1	100416	-	8.08	0.009	0.11	8.08	0.00
14	K&Z CHP1	060495	-	10.17	0.008	0.08	9.45	7.62
14	K&Z CHP1	110656	-	7.61	0.009	0.12	7.56	0.66
14	K&Z CHP1	110686	-	7.76	0.011	0.15	7.73	0.39
14	K&Z CHP1	80001	-	8.03	0.005	0.07	8.07	-0.50
14	K&Z CHP1	80028	-	8.14	0.009	0.11	8.19	-0.61
14	K&Z CHP1	110657	PT 100 not connected Calibrated also in 2016	7.66	0.007	0.09	7.61	0.66
14	K&Z CH1	020288	Calibrated also in 2016	10.2	0.011	0.10	10.24	-0.39
14	K&Z CH1	070574	Calibrated also in 2016	9.31	0.010	0.11	9.36	-0.53
14	Eppley Nip	35818E6	Calibrated also in 2016	8.08	0.023	0.28	8.15	-0.86
14	Eppley Nip	20119E6	Calibrated also in 2015 and 2016	8.38	0.026	0.31	8.12	3.20
14	Eppley Nip	21131E6	-	7.94	0.042	0.52	7.98	-0.50
14	Eppley Nip	30404E6	-	8.42	0.041	0.48	8.42	0.00
14	Eppley Nip	31125E6	-	8.81	0.037	0.43	8.79	0.23

14	Eppley Nip	29542E6	Calibrated also in 2015 and 2016	8.23	0.040	0.48	8.22	0.12
14	Eppley Nip	29015E6	-	8.84	0.029	0.32	8.94	-1.12
14	Eppley Nip	27569E6	-	8.61	0.029	0.34	8.76	-1.71
14	Eppley Nip	37123E6	-	7.99	0.022	0.28	8.04	-0.62
14	Eppley Nip	28056E6	-	8.45	0.033	0.39	8.51	-0.71
15	K&Z CHP1	090121	Calibrated also in 2016	7.97	0.006	0.08	7.94	0.38
15	K&Z CHP1	100236	-	7.78	0.012	0.16	7.84	-0.77
15	K&Z CHP1	110779	-	7.61	0.010	0.13	7.57	0.53
15	K&Z CHP1	110780	-	7.82	0.011	0.14	7.85	-0.38
15	K&Z CHP1	090167	PT 100 not connected	7.72	0.007	0.09	7.71	0.13
15	K&Z CH1	040381	-	10.89	0.012	0.11	10.87	0.18
15	K&Z CH1	080002	-	9.6	0.029	0.30	9.73	-1.34
15	Eppley Nip	20004E6	Calibrated also in 2016	7.74	0.030	0.38	7.77	-0.39
15	Eppley Nip	23338E6	Calibrated also in 2016	9.2	0.050	0.54	9.27	-0.76
15	Eppley Nip	18949E6	-	8.74	0.032	0.37	7.97	9.66
15	Eppley Nip	29542E6	Calibrated also in 2014 and 2016	8.23	0.043	0.52	8.23	0.00
15	Eppley Nip	35422E6	-	8.35	0.017	0.20	8.4	-0.60
15	Eppley Nip	20119E6	Calibrated also in 2014 and 2016	8.42	0.028	0.33	8.38	0.48
15	Eppley Nip	36895E6	-	8.15	0.025	0.31	8.24	-1.09
15	Hukseflux DR02	9089	Calibrated also in 2016	9.25	0.019	0.20	9.31	-0.64
16	K&Z CHP1	090163	-	7.95	0.015	0.18	7.98	-0.38
16	K&Z CHP1	110657	Calibrated also in 2014	7.64	0.012	0.16	7.66	-0.26
16	K&Z CHP1	110742	-	7.4	0.010	0.13	7.39	0.14
16	K&Z CHP1	090164	Temperature signal of PT100 faulty (about 20°C to much)	7.97	0.013	0.17	8.04	-0.87
16	K&Z CHP1	090121	Calibrated also in 2015	7.97	0.011	0.14	7.97	0.00
16	K&Z CHP1	120880	Connected to BlackPhoton sun tracker and DAS	7.65	0.011	0.14	7.62	0.39
16	K&Z CH1	070574	Calibrated also in 2014	9.28	0.020	0.22	9.31	-0.32
16	K&Z CH1	020288	Calibrated also in 2014	10.19	0.015	0.14	10.2	-0.10
16	K&Z CH1	010270	-	10.19	0.019	0.19	10.06	1.29
16	Eppley Nip	29542E6	Calibrated also in 2014 and 2015	8.19	0.036	0.44	8.23	-0.49
16	Eppley Nip	35818E6	Calibrated also in 2014	8.07	0.027	0.33	8.08	-0.12
16	Eppley Nip	23338E6	Calibrated also in 2015	9.17	0.047	0.52	9.2	-0.33

16	Eppley Nip	20119E6	Calibrated also in 2014 and 2015	8.39	0.027	0.32	8.42	-0.36
16	Eppley Nip	20004E6	Calibrated also in 2015 campaign	7.72	0.034	0.45	7.74	-0.26
16	Eppley Nip	21626E6	-	8.4	0.041	0.49	8.5	-1.18
16	Hukseflux DR02	9089	Calibrated also in 2015 campaign	9.25	0.023	0.25	9.25	0.00
16	Hukseflux DR03	10025	Connected to BlackPhoton sun tracker and DAS	10.12	0.011	0.11	10.11	0.10

Table 4 lists the average deviation and absolute average deviation of the newly derived responsivity compared to the most recent older responsivity. Only sensors which are calibrated for the first time at the PSA, sensor calibration results of second or third appearance are not considered in this table.

The older K&Z CH1 and Eppley Nip sensors were not calibrated for many years and show a general decrease of the responsivity >0.5%. Looking into the absolute average deviation of all sensors no strong fluctuations in between the campaigns were observed. This is also the case if only the 16 individual K&Z CHP1 sensors are considered. The K&Z CH1 (5 individual devices) and Eppley Nip (16 individual devices) sensors show stronger fluctuation in between the campaigns, mainly triggered by a few sensors with absolute deviations larger 1%. In most cases with absolute deviations larger 1% the responsivity decreased, which can be explained by aging processes of the thermopile of these older pyrheliometer models. Since the Hukseflux sensors are only represented by two devices from different models, no statistically significant statement is possible. As expected is an overall decrease of the responsivity observed, triggered by a degradation processes of the thermopiles over time.

A responsivity value was calculated for each series and device of the valid data. All obtained responsivities were averaged to calculate the final responsivity of a device. The rsd for the responsivity was calculated according to Equation 1. No significant changes of the signal noise changes in between the campaigns were observed. The K&Z CHP1 sensors showed with an average rsd of 0.12% the most stable operation.

Table 4. **average deviation and absolute average deviation to most recent older responsivities (Only the sensors first appearance at a PSA calibration campaign; without outlier sensors) and average rsd of new responsivity (pyrheliometer)**

	Avg. dev. to most recent older responsivity in %				Abs. avg. dev. to most recent older responsivity in %				Avg. rsd of new responsivity in %			
Year	**14**	**15**	**16**	**all**	**14**	**15**	**16**	**all**	**14**	**15**	**16**	**all**
All sensors	-0.32	-0.39	-0.30	-0.34	0.56	0.60	0.51	0.57	0.25	0.26	0.26	0.26
K&Z CHP1	0.10	-0.02	-0.18	-0.02	0.47	0.44	0.44	0.45	0.10	0.12	0.15	0.12
K&Z CH1	-0.46	-0.58	-	-0.52	0.46	0.76	-	0.61	0.11	0.20	0.18	0.17
Eppley Nip	-0.57	-0.71	-1.18	-0.66	0.65	0.71	1.18	0.71	0.38	0.38	0.42	0.39
Hukseflux DR02/3	-	-0.64	0.10	-0.27	-	0.64	0.10	0.37	-	0.20	0.18	0.19

Ten devices were calibrated more than once during the three PSA campaigns. The responsivity and the deviation to the most recent older responsivity for these sensors in listed in Table 5. No significant changes in responsivity in between the campaigns were observed. In fact all the observed absolute deviations for repeatedly calibrated sensors are significantly lower than the absolute average deviation stated in Table 4. This is explained basically by the fact that some of the sensors were not calibrated for several years before their first calibration at PSA. Many sensors were not used for measuring data but they were mounted in the field, at times even on a solar tracker.

Table 5. **Responsivities and deviation to most recent older responsivity for repeatedly calibrated sensors (pyrheliometer)**

Device	Original manufacturer calibration	2014	2015	2016
CHP1 SN: 110657	7.61 µV/(W/m²)	7.66 µV/(W/m²)	-	7.64 µV/(W/m²)
	-	0.66%	-	-0.26%
CHP1 SN: 090121	7.94 µV/(W/m²)	-	7.97 µV/(W/m²)	7.97 µV/(W/m²)
	-	-	0.38%	0.00%
CH1 SN: 020288	10.24 µV/(W/m²)	10.20 µV/(W/m²)	-	10.19 µV/(W/m²)
	-	-0.39%	-	-0.10%
CH1 SN: 070574	9.36 µV/(W/m²)	9.31 µV/(W/m²)	-	9.28 µV/(W/m²)
	-	-0.53%	-	-0.32%
Nip SN: 35818E6	8.15 µV/(W/m²)	8.08 µV/(W/m²)	-	8.07 µV/(W/m²)
	-	-0.86%	-	-0.12%
Nip SN: 20119E6	8.12 µV/(W/m²)	8.38 µV/(W/m²)	8.42 µV/(W/m²)	8.39 µV/(W/m²)
	-	3.20%	0.48%	-0.36%
Nip SN: 29542E6	8.22 µV/(W/m²)	8.23 µV/(W/m²)	8.23 µV/(W/m²)	8.19 µV/(W/m²)
	-	0.12%	0.00%	-0.49%
Nip SN: 20004E6	7.77 µV/(W/m²)	-	7.74 µV/(W/m²)	7.72 µV/(W/m²)
	-	-	-0.39%	-0.26%
Nip SN: 23338E6	9.27 µV/(W/m²)	-	9.20 µV/(W/m²)	9.17 µV/(W/m²)
	-	-	-0.76%	-0.33%
DR02 SN: 9089	9.31 µV/(W/m²)	-	9.25 µV/(W/m²)	9.25 µV/(W/m²)
	-	-	-0.64%	0.00%

4.3 Results of the pyranometer calibrations with continuous sun-and-shade method

4.3.1 Obtained valid DNI and DHI reference

After the data pre-processing, data are filtered. The following filters were active (in this order):

- DNI<300 W/m²
- DHI>300 W/m²
- DHI fluctuation >5%/min
- DHI fluctuation >1%/10sec
- Wind from sun azimuth ±30° with wind speed larger 5 m/s
- Due to influence of clouds (METAS cloud camera)
    - Angular distance to sun >15°
- Series with less than 10 valid measurement values
- All time stamps with a Rij which deviate by more than 5 % from their series Rj,
    - Actual wording in ISO 9846 reads “Eliminate from the calculation all sets which deviate from the corresponding series mean by more than 5%”. Since this is placed in the standard before the actual responsivity calculation, this can be interpreted as a filter for the actual GHI signal and not the corresponding responsivity. Using this filter on the actual GHI signal would lead to a complete loss of all data taken in the morning and evening when the sun elevation is changing rapidly. Wording should be changed in a more precise matter, which doesn’t give so much space for interpretation.
- Series are entirely rejected if more than 50 % of its values have been eliminated

For pyranometer calibration with the continuous shade method the standard ISO 9846 requires that the variation of the DHI caused by cloud movement is less than 1 % in 10 seconds. This statement from the standard can be understood in different ways. We evaluate it with three different criteria in order to exclude as much inadequate data as possible. Only if all three tests are passed the data is used for the calibration. The first test is to evaluate the 2-second average DHI measurements contributing to the 10-second averages that are used in the calibration. If the difference between the maximum and the minimum of the 2-second DHI measurements is greater than 1 % of the 10-second average the 10-second average is excluded. This is not sufficient in our opinion as the response time of the reference pyranometers is 5 seconds (95 % signal level). Hence, we also investigate the change of the 10-second DHI averages. If the change is greater than 1 % for two consecutive DHI 10-second averages both values are excluded. The third test is to investigate the temporal gradient of the DHI between two reference DHI measurements that are obtained in parallel to the ACR readings. ACR readings are obtained only every 2 minutes. If the gradient is greater than 1 % per 10 seconds the data is excluded, too.

Figure 9, Figure 10 and Figure 11 illustrate the DNI and DHI reference signals and the filters causing the data rejection. They also list the share of the individual filters. For the 2014 and 2016 more than 60% of the initial data is considered as valid. Due to bad wetter conditions with a strong influence from many scattered clouds less than 17% of the initial data are considered as valid for the 2015 calibration.

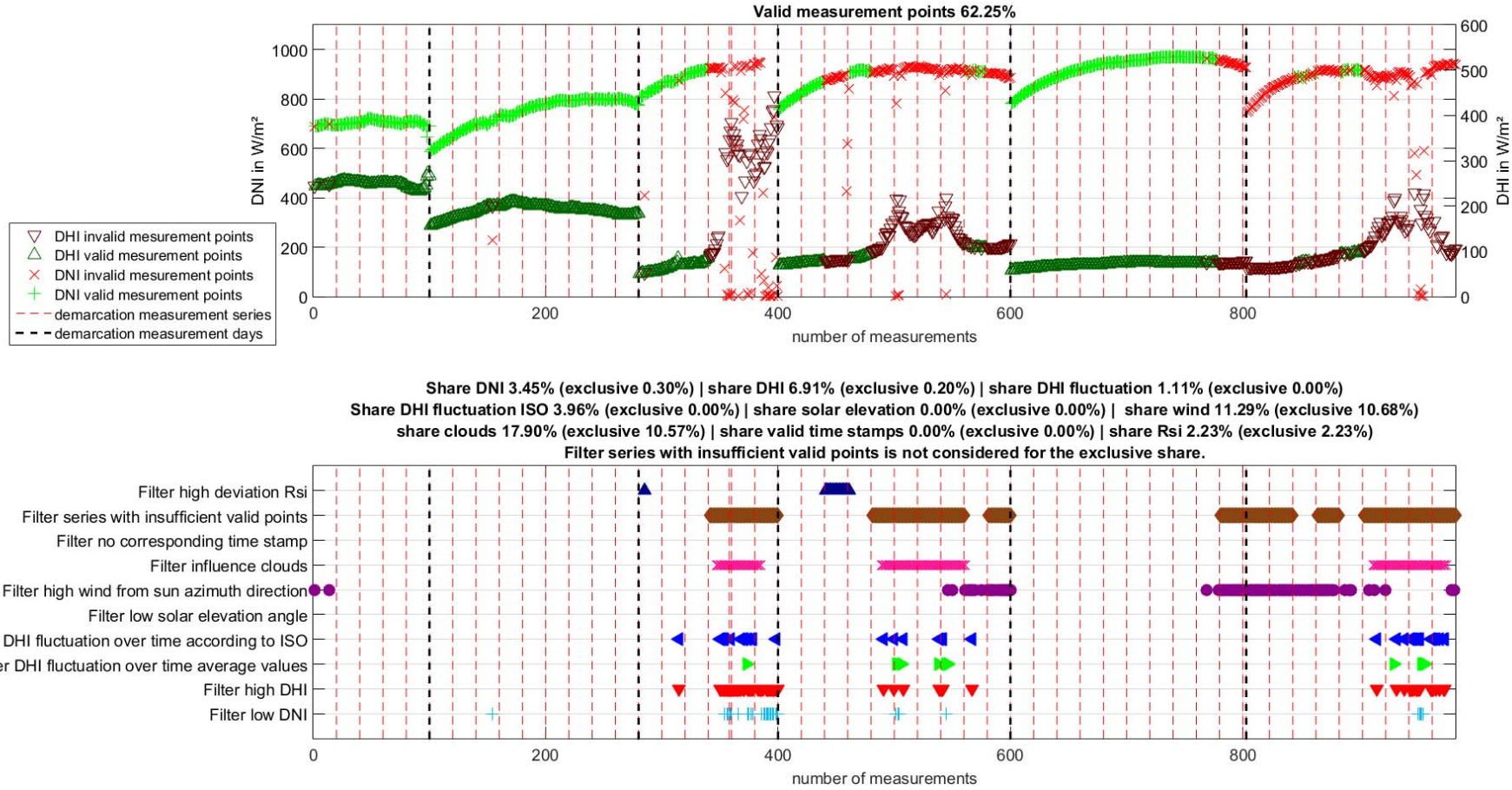

Figure 9. **2014 pyranometer campaign; Top) valid and invalid reference data; Bottom) marker for active filter of the invalid data**

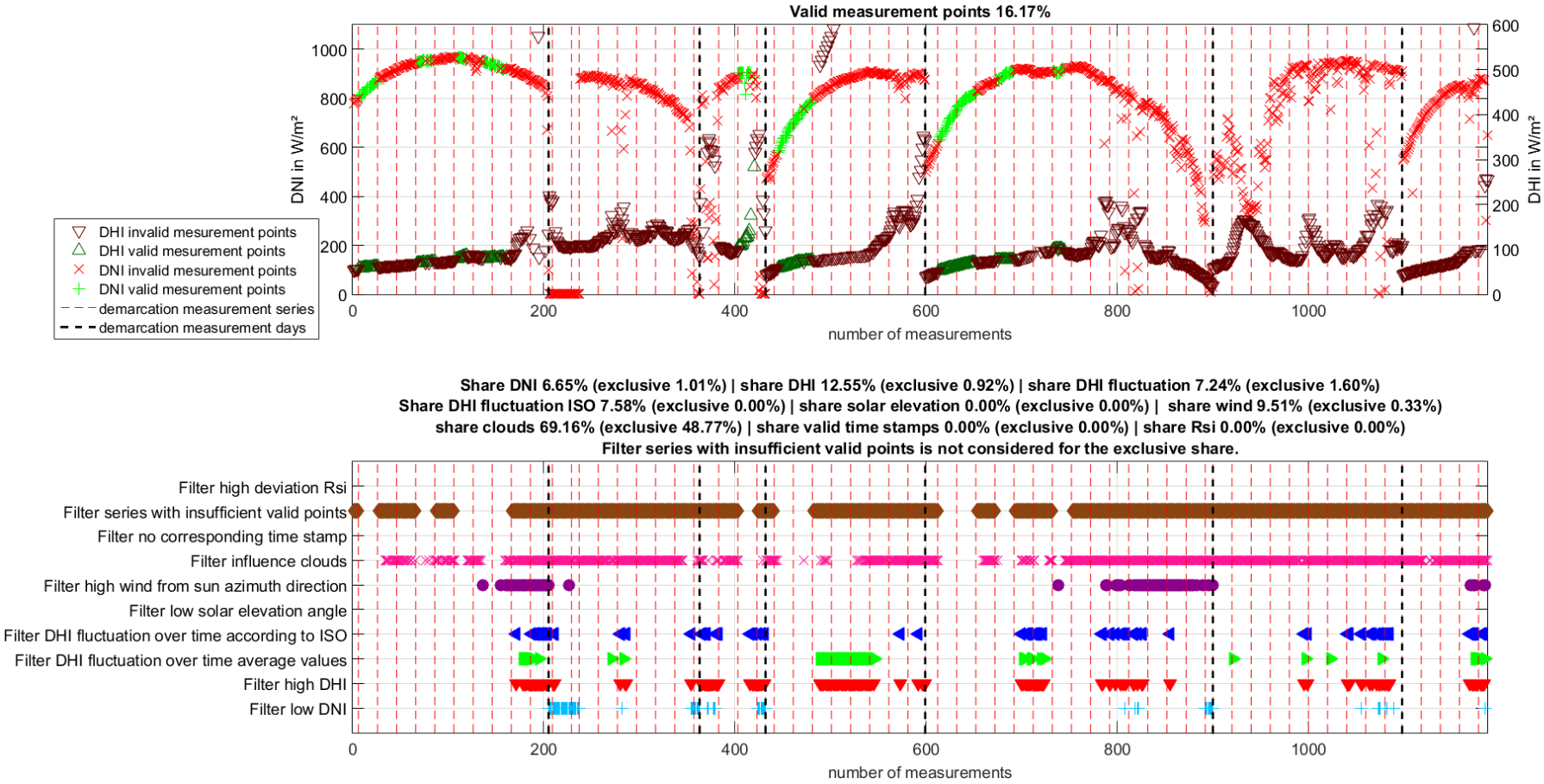

Figure 10. **2015 pyranometer campaign; Top) valid and invalid reference data; Bottom) marker for active filter of the invalid data**

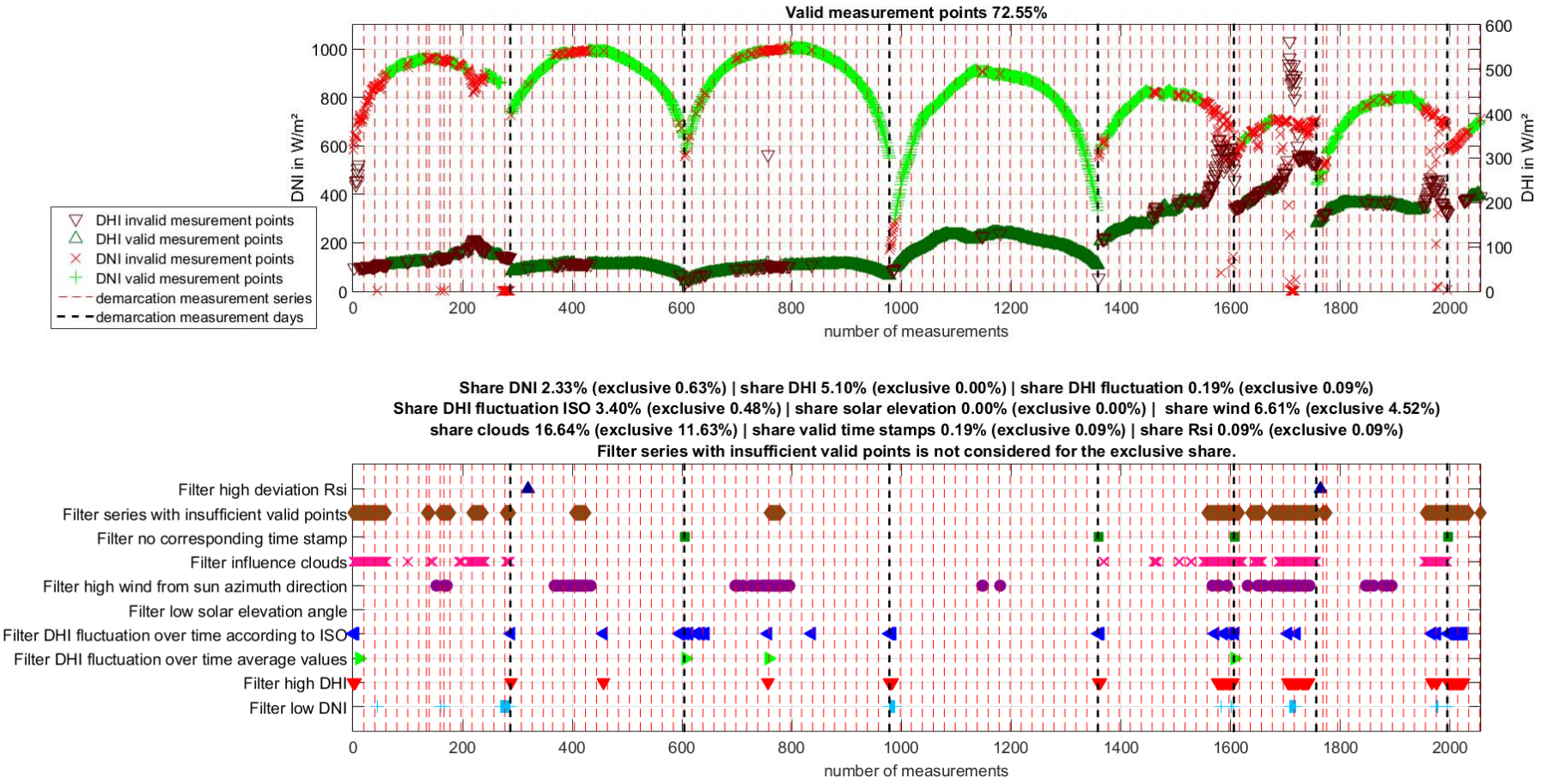

Figure 11. **2016 pyranometer campaign; Top) valid and invalid reference data; Bottom) marker for active filter of the invalid data**

4.3.2 Discussion of Pyranometer results continuous sun-and-shade method

A total of 29 new responsivities distributed over 27 individual field pyranometers were derived from the measurement data (2xCMP22, 16xCMP21, 1xCM21, 1xCMP11, 6xCM11 and 1x SR12-T1-05). Table 6 list all field pyranometers, which were participating at the PSA calibration campaigns. Some sensors were repeatedly in varies campaigns calibrated. In most cases only small deviations between the new responsivity and the responsivity from the last calibration are small and explainable with a drift of 1%/year.

While comparing old and new responsivities with each other, it has to be considered that the manufacturer use mainly laboratory calibration with artificial light source placed at the zenith of the sensor, thus deviations can also arise due to angle dependences of the pyranometers. The angle dependence of the pyranometer will be discussed in more detail in chapter 4.3.2.1.

For the four sensors CMP21_090292, CMP21_090280, CMP21_090281 and CMP21_090279 the newly derived responsivity showed large deviations >2% to the previous responsivity (see Table 6). A detailed discussion of the historical sensor responsivity evolution for these sensors is given in chapter 4.3.2.2, for the further statistics in this chapter these sensors are considered as outliers.

Table 6. **List on calibration campaigns participating field pyranometer with results for new responsivities**

year	Model	Serial number	Comment	New responsivity in µV/(W/m²)	Std of new responsivity in µV/(W/m²)	Rsd of new responsivity in %	Old responsivity in µV/(W/m²)	Deviation to most recent older responsivity in %
14	K&Z CMP21	110790	ventilation unit	9.5	0.032	0.34	9.37	1.39
14	K&Z CMP21	110789	ventilation unit	9.84	0.026	0.26	9.84	0.00
14	K&Z CMP21	080142	ventilation unit	8.75	0.131	1.50	8.71	0.46
14	K&Z CMP11	070357	-	8.61	0.093	1.08	8.58	0.35
14	K&Z CM11	871856	-	4.77	0.043	0.90	4.77	0.00
14	K&Z CM11	851120	-	5.18	0.042	0.82	5.17	0.19
14	K&Z CM11	007346	-	5.13	0.050	0.97	5.08	0.98
14	K&Z CM11	851123	-	4.82	0.048	0.99	4.81	0.21
14	K&Z CM11	924494	-	4.38	0.051	1.17	4.36	0.46
15	K&Z CMP22	140047	Calibrated also in 2016	10.31	0.029	0.28	10.23	0.78
15	K&Z CMP21	110868	-	10.17	0.096	0.95	10.14	0.30
15	K&Z CMP21	110876	ventilation unit	9.44	0.049	0.52	9.41	0.32
15	K&Z CMP21	90300	-	9.11	0.012	0.13	9.04	0.77
15	K&Z CMP21	90291	-	8.53	0.059	0.69	8.54	-0.12
15	K&Z CMP21	110869	-	9.38	0.035	0.38	9.35	0.32
15	K&Z CMP21	110875	-	9.99	0.103	1.03	10.06	-0.70

15	K&Z CM21	041275	Calibrated also in 2016 n	11.24	0.139	1.24	11.22	0.18
15	SR12-T1-05	1183	-	14.19	0.076	0.54	13.94	1.79
16	K&Z CMP22	160418	-	9.88	0.048	0.48	9.84	0.41
16	K&Z CMP22	140047	Calibrated also in 2015	10.32	0.027	0.26	10.31	0.10
16	K&Z CMP21	090292	-	8.53	0.033	0.39	8.3	2.77
16	K&Z CMP21	110846	-	8.55	0.030	0.35	8.46	1.06
16	K&Z CMP21	110845	-	8.97	0.044	0.49	8.86	1.24
16	K&Z CMP21	070133	ventilation unit	8.48	0.029	0.35	8.4	0.95
16	K&Z CMP21	090280	ventilation unit	9.19	0.043	0.47	8.98	2.34
16	K&Z CMP21	090281	ventilation unit	9.77	0.058	0.59	9.47	3.17
16	K&Z CMP21	090279	ventilation unit	8.86	0.058	0.65	8.58	3.26
16	K&Z CM21	041275	Calibrated also in 2015	11.4	0.042	0.37	11.24	1.42
16	K&Z CM11	027716	-	5.1	0.028	0.55	5.02	1.59

Table 8 lists the average deviation and absolute average deviations of the newly derived responsivity compared to the most recent older responsivity. Only sensors which are calibrated for the first time at the PSA, sensor calibration results of second or third appearance are not considered in this table.

Almost no deviation between the average deviation and absolute average deviations are present. With the exception of two sensors are the responsivities obtained during the PSA calibration always higher than the manufacturer responsivities. This is also the case for PSA responsivities generated with a data set that includes only zenith angles <19°, which rather corresponds to the manufacturer's calibration with an artificial light source positioned at the zenith of the sensor (see chapter 4.3.2.1). Thus a permanent overestimation of the measurement signal is expected using the manufacturer responsivity without any further correction.

Looking into the deviation over all sensors (see Table 7), fluctuations around 0.5% in between the campaigns were observed. Especially in 2016 were for some sensors higher deviations observed. At the same time are the overall rsd values with 0.45% lowest at the 2016 campaign. A possible reason for that might be the improved pyranometer test stand introduced in the 2016 campaign, which might be less sensitive for sensor alignment errors than the previously used pyranometer table.

In general is a decrease of the responsivity expected, triggered by degradation processes of the thermopiles over time. But the results stated in Table 7 show an average increase of the responsivity. At the first glance this raises the question of systematically error which occurs during the calibration procedure (including data processing). However the authors of this report think that the reason for this unexpected raise of the responsivity lies with the calibration of the manufacturers (mainly Kipp&Zonen). DLR and Ciemat operate with international partners varies meteorological stations around the world. Verification of the DNI coincidence is part of the daily data check routine of these stations. DNI coincidence compares the measured DNI with the calculated DNI based on GHI and DHI measurements (see Equation 2).

Equation 2

$$DNIcoincidence = DNI - \left(\frac{GHI - DHI}{cos(SZA)}\right)$$

In all stations operated the calculated DNI is higher than the measured DNI. A typical DNI coincidence of a clear sky day is illustrated in Figure 12. This effect might be explained by a to low manufacturer responsivity of the pyranometers which leads to overrated GHI and DHI values which would also explain the increase of the responsivity observed at PSA field calibration.

Table 7. **Absolute average deviation to most recent older responsivities (Only the sensors first appearance at a PSA calibration campaign; without outlier sensors) and average rsd of new responsivity (pyranometer)**

	Avg. dev. to most recent older responsivity in %				Abs. avg. dev. to most recent older responsivity in %				Avg. rsd of new responsivity in %			
	2014	**2015**	**2016**	**all**	**2014**	**2015**	**2016**	**all**	**2014**	**2015**	**2016**	**all**
All sensors	0,45	0,41	0,67	0,56	0,45	0,59	0,84	0,63	0,89	0,64	0,45	0,65
K&Z CMP22	-	0,78	0,41	0,59	-	0,78	0,41	0,59	-	0,28	0,37	0,34
K&Z CM/P21	0,62	0,15	1.09	0,48	0,62	0,39	1.09	0,60	0,70	0,70	0.46	0,59
K&Z CM/P11	0,37	-	1,59	0,54	0,37	-	1,59	0,54	0,99	-	0,55	0,93
Huksefl ux SR12	-	1,79	-	1,79	-	1,79	-	1,79	-	0,54	-	0,54

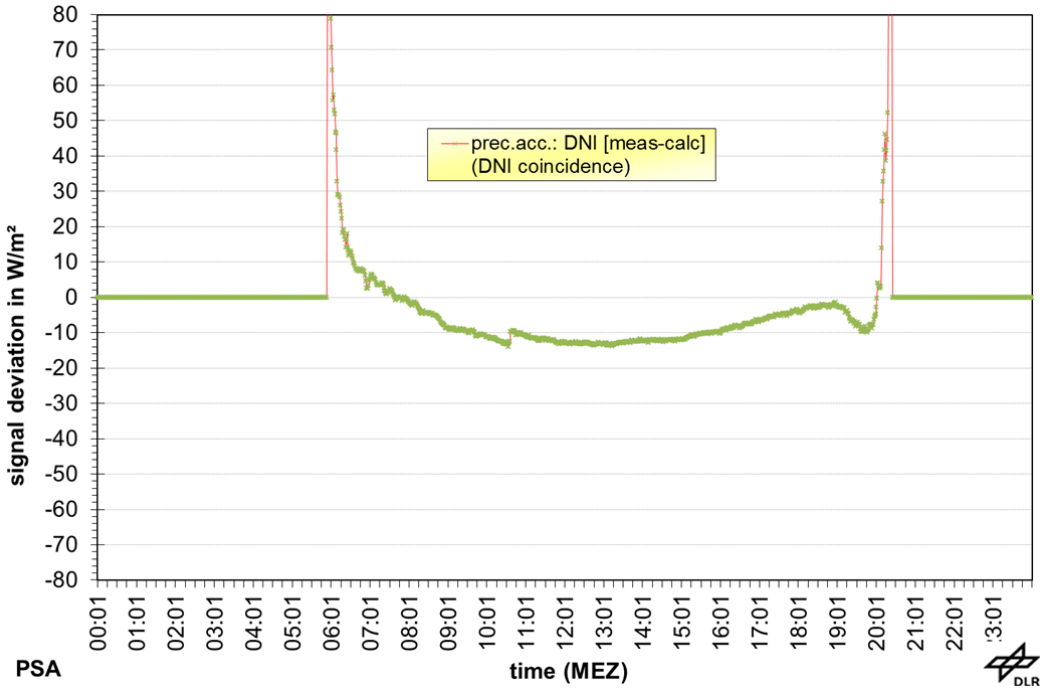

Figure 12. **Typical DNI-coincidence of clear sky day measured at the DLR PSA HP meteorological station**

Only two pyranometers were repeatedly calibrated during the three PSA campaigns. The responsivity and the deviation to the most recent older responsivities for these sensors in listed in Table 8. The CMP22 sensor shows only a deviation of 0.1 % between the 2015 and 2016 campaign. The second sensor received a new responsivity in 2015 which deviated by only 0.18% from the previous most recent responsivity, but the 2016 responsivity deviates for more than 1.4% from 2015 responsivity. The unusual raise in responsivity cannot be explained by the authors of this report, since the calibration and operation history of this sensor is not well documented.

Table 8. **Responsivities and deviation to most recent older responsivity for repeatedly calibrated sensors (pyranometer)**

	Original manufacturer calibration	2014	2015	2016
Device : CMP22 SN: 140047	10.23 µV/(W/m²)	-	10.31 µV/(W/m²)	10.32 µV/(W/m²)
	-	-	0.78%	0.10%
Device : CM21 SN: 041275	11.22 µV/(W/m²)	-	11.24 µV/(W/m²)	11.40 µV/(W/m²)
	-	-!	0.18%	1.42%

4.3.2.1 Solar zenith and azimuth angle dependency of pyranometer responsivity

For the data of the 2016 campaign the sun position dependency on the pyranometer responsivity was studied. All pyranometers were aligned with the cable pointing to north. Since the responsivity was calculated for each data point separately a high angular dependent responsivity resolution is available. The angle dependent responsivities are listed in Table 9. The responsivity fluctuates around 0.5 percentage points between forenoon and afternoon at solar zenith angle up to 60°. For solar zenith angle up to 60° the fluctuations rise up to 2.7 percentage points (at zenith angle 80°). The average responsivities of forenoon and afternoon deviate up to 0.3 percentage points from the overall average responsivity for zenith angles up to 60°.

The manufacturer responsivity can be best compared with the responsivity derived from the min SZA (in this case 13.7°), since the manufacturers use an artificial light source positioned at the zenith of the sensor for the calibration. Table 10 lists the responsivities and deviations. The field calibrations result in every case in a higher responsivity. The particularly high deviation of four sensors will be investigated in more detail in chapter 4.3.2.2.

Table 9. **Pyranometer solar azimuth and zenith angle dependent responsivities in µV/(W/m²) and deviation in % (only 2016 campaign)**

		CM21_041 275	CMP22_160 418	CMP21_090 292	CMP22_140 047	CMP21_110 846	CMP21_110 845	CM11_027 716	CMP21_070 133	CMP21_090 280	CMP21_090 281	CMP21_090 279
Responsivity avg.		11,40	9,88	8,53	10,32	8,55	8,97	5,10	8,48	9,19	9,77	8,86
Responsivity SZA 13,7°	AM&PM	11,38	9,90	8,55	10,30	8,56	8,97	5,09	8,51	9,19	9,73	8,83
		0,18%	**-0,20%**	**-0,23%**	**0,19%**	**-0,12%**	**0,00%**	**0,20%**	**-0,35%**	**0,00%**	**0,41%**	**0,34%**
Responsivity SZA 40°	AM	11,42	9,91	8,53	10,31	8,56	8,96	5,10	8,47	9,19	9,78	8,87
		-0,18%	**-0,30%**	**0,00%**	**0,10%**	**-0,12%**	**0,11%**	**0,00%**	**0,12%**	**0,00%**	**-0,10%**	**-0,11%**
	PM	11,37	9,87	8,54	10,33	8,56	9,00	5,08	8,48	9,17	9,72	8,83
		0,26%	**0,10%**	**-0,12%**	**-0,10%**	**-0,12%**	**-0,33%**	**0,39%**	**0,00%**	**0,22%**	**0,51%**	**0,34%**
	AM&PM	11,40	9,89	8,54	10,32	8,56	8,98	5,09	8,48	9,18	9,75	8,85
		0,04%	**-0,10%**	**-0,06%**	**0,00%**	**-0,12%**	**-0,11%**	**0,20%**	**0,06%**	**0,11%**	**0,20%**	**0,11%**
Responsivity SZA 45°	AM	11,43	9,91	8,53	10,32	8,56	8,97	5,11	8,47	9,19	9,79	8,87
		-0,26%	**-0,30%**	**0,00%**	**0,00%**	**-0,12%**	**0,00%**	**-0,20%**	**0,12%**	**0,00%**	**-0,20%**	**-0,11%**
	PM	11,37	9,87	8,54	10,33	8,57	9,01	5,08	8,48	9,18	9,73	8,83
		0,26%	**0,10%**	**-0,12%**	**-0,10%**	**-0,23%**	**-0,45%**	**0,39%**	**0,00%**	**0,11%**	**0,41%**	**0,34%**
	AM&PM	11,40	9,89	8,54	10,33	8,57	8,99	5,10	8,48	9,19	9,76	8,85
		0,00%	**-0,10%**	**-0,06%**	**-0,05%**	**-0,18%**	**-0,22%**	**0,10%**	**0,06%**	**0,05%**	**0,10%**	**0,11%**

		CM21_041275	CMP22_160418	CMP21_090292	CMP22_140047	CMP21_110846	CMP21_110845	CM11_027716	CMP21_070133	CMP21_090280	CMP21_090281	CMP21_090279
Responsivity avg.		11,40	9,88	8,53	10,32	8,55	8,97	5,10	8,48	9,19	9,77	8,86
Responsivity SZA 60°	AM	11,45	9,88	8,49	10,31	8,54	8,94	5,12	8,45	9,21	9,82	8,90
		-0,44%	**0,00%**	**0,47%**	**0,10%**	**0,12%**	**0,33%**	**-0,39%**	**0,35%**	**-0,22%**	**-0,51%**	**-0,45%**
	PM	11,38	9,84	8,53	10,34	8,53	9,02	5,07	8,48	9,22	9,75	8,85
		0,18%	**0,40%**	**0,00%**	**-0,19%**	**0,23%**	**-0,56%**	**0,59%**	**0,00%**	**-0,33%**	**0,20%**	**0,11%**
	AM&PM	11,42	9,86	8,51	10,33	8,54	8,98	5,10	8,47	9,22	9,79	8,88
		-0,13%	**0,20%**	**0,23%**	**-0,05%**	**0,18%**	**-0,11%**	**0,10%**	**0,18%**	**-0,27%**	**-0,15%**	**-0,17%**
Responsivity SZA 70°	AM	11,48	9,83	8,46	10,30	8,52	8,88	5,14	8,44	9,20	9,86	8,94
		-0,70%	**0,51%**	**0,82%**	**0,19%**	**0,35%**	**1,00%**	**-0,78%**	**0,47%**	**-0,11%**	**-0,92%**	**-0,90%**
	PM	11,37	9,82	8,51	10,36	8,51	9,04	5,07	8,49	9,16	9,79	8,90
		0,26%	**0,61%**	**0,23%**	**-0,39%**	**0,47%**	**-0,78%**	**0,59%**	**-0,12%**	**0,33%**	**-0,20%**	**-0,45%**
	AM&PM	11,43	9,83	8,49	10,33	8,52	8,96	5,11	8,47	9,18	9,83	8,92
		-0,22%	**0,56%**	**0,53%**	**-0,10%**	**0,41%**	**0,11%**	**-0,10%**	**0,18%**	**0,11%**	**-0,56%**	**-0,68%**
Responsivity SZA 80°	AM	11,50	9,70	8,45	10,36	8,54	8,98	5,23	8,47	9,33	10,00	9,08
		-0,88%	**1,82%**	**0,94%**	**-0,39%**	**0,12%**	**-0,11%**	**-2,55%**	**0,12%**	**-1,52%**	**-2,35%**	**-2,48%**
	PM	11,32	9,84	8,49	10,44	8,49	9,07	5,07	8,51	8,95	9,88	8,99
		0,70%	**0,40%**	**0,47%**	**-1,16%**	**0,70%**	**-1,11%**	**0,59%**	**-0,35%**	**2,61%**	**-1,13%**	**-1,47%**
	AM&PM	11,41	9,77	8,47	10,40	8,52	9,03	5,15	8,49	9,14	9,94	9,04
		-0,09%	**1,11%**	**0,70%**	**-0,78%**	**0,41%**	**-0,61%**	**-0,98%**	**-0,12%**	**0,54%**	**-1,74%**	**-1,98%**

Table 10. **Pyranometer min zenith angle responsivities compared with most recent manufacturer responsivities in μV/(W/m²) and deviation in % (only 2016 campaign)**

		CM21_041275	CMP22_160418	CMP21_090292	CMP22_140047	CMP21_110846	CMP21_110845	CM11_027716	CMP21_070133	CMP21_090280	CMP21_090281	CMP21_090279
Manufacturer responsivity		11,24	9,84	8,3	10,23	8,46	8,86	5,02	8,4	8,98	9,47	8,58
Responsivity SZA 13,7°	AM&PM	11,38	9,90	8,55	10,30	8,56	8,97	5,09	8,51	9,19	9,73	8,83
		-1,25%	**-0,61%**	**-3,01%**	**-0,68%**	**-1,18%**	**-1,24%**	**-1,39%**	**-1,31%**	**-2,34%**	**-2,75%**	**-2,91%**

4.3.2.2 Detailed discussion of historical sensor responsivity evolution for some sensors

For the four DLR devices CMP21_090292, CMP21_090280, CMP21_090281 and CMP21_090279, which participated on the 2016 campaign, a deviation >2% between the newly obtained responsivity and the most recent manufacturer responsivity was detected. All four sensors were calibrated for the first time by Kipp&Zonen within the same week in November 2009 and all sensors were recalibrated on the 15th of May in 2013 (see Table 11). In the table the new responsivity of these sensors from the calibration at PSA is compared to the 2013 Kipp&Zonen calibration. The calibration results PSA results are much closer to Kipp&Zones's results from 2009 in all four cases. The observed deviation is almost halved, when the new responsivity is compared to the Kipp&Zonen calibration of 2009. This suggests a systematically too low result of the Kipp&Zonen calibrations on 15th of May in 2013.

In order to further investigate the deviations nearly two years of measurement data from PSA were used. During the time period between 30th of May 2014 and 10th of March 2016 two of the pyranometers were used at the DLR PSA HP meteorological station. The CMP21_090292 measured DHI, the CMP21_090281 measured GHI and the CHP1_090163 measured DNI.

For every single day a data verification check is done. Part of this check is the comparison of the measured DNI with the calculated DNI. For this purpose the DNI-coincidence is calculated according to Equation 2.

During the first 6 months of this time period an unusually high DNI-coincidence around -25 W/m² in average was observed (solar noon ±1° solar azimuth). To resolve this issue, the responsivity of the devices CMP21_090292 and CMP21_090281 were adjusted. The reference data from the first joint calibration campaign from June 2014 were used. The devices CMP21_090292 and CMP21_090281 were not part of the calibration campaign, but they were operated in a distance of about 500 m from the calibration site at this time. This procedure, which is not compliant with the standard ISO 9846, changed the original responsivities from 2013 by about -2 % and reduced the average DNI-coincidence below -10 W/m². The deviation of these responsivities derived from the 2014 calibration campaign compared to the Kipp&Zonen responsivity from 2009 are below 1% and around 1% compared to the new derived responsivity from the 2016 campaign. Figure 13 and Figure 14 show the impact of different responsivities on the DNI-coincidence. The following quantities are plotted over time:

- Blue (Responsivity HP): DNI-coincidence calculated with corrected data directly from the HP meteorological station data base (for the first half of data period only the responsivity of the GHI signal was corrected; for the second half both GHI and DHI signal were corrected)
- Orange (Responsivity K&Z 2013): DNI-coincidence resulting with K&Z responsivities from 2013 calibration
- Yellow (Responsivity DLR 2015): DNI-coincidence resulting with PSA calibration derived in 2015 with data from 2014 campaign (used for HP meteorological station correction)
- Purple (Responsivity DLR 2016): DNI-coincidence resulting with responsivities from 2016 PSA calibration campaign
- Green: Fit over time between DLR 2015 and DLR 2016

For every single time stamp the highest DNI-coincidence values result while using the K&Z 2013 Responsivities.

The responsivity of the CHP1_090163 for the DNI signal is documented in Table 12 and no unusual changes are observed. The described observations suggest, that the Kipp&Zonen pyranometer

calibrations from 2013 for the devices CMP21_090292, CMP21_090280, CMP21_090281 and CMP21_090279 yielded systematically too low responsivities.

Table 11. **Calibration history of the field pyranometers CMP21_090292, CMP21_090280, CMP21_090281 and CMP21_090279**

Device: CMP21| SN.: 090292				
Calibrated by	K&Z	K&Z	PSA	PSA
Calibrated Date	10.11.2009	15.05.2013	05.03.2015	30.06.2016
Responsivity in µV/(W/m²)	8.42	8.3	8.45	8.53
Deviation to most recent older responsivity in %	-	-1.43	1.81	0.95
Device: CMP21| SN.: 090280				
Calibrated by	K&Z	K&Z	-	PSA
Calibrated Date	04.11.2009	15.05.2013	-	30.06.2016
Responsivity in µV/(W/m²)	9.05	8.98	-	9.19
Deviation to most recent older responsivity in %	-	-0.77	-	2.35
Device: CMP21| SN.: 090281				
Calibrated by	K&Z	K&Z	PSA	PSA
Calibrated Date	04.11.2009	15.05.2013	05.03.2015	30.06.2016
Responsivity in µV/(W/m²)	9.58	9.47	9.66	9.77
Deviation to most recent older responsivity in %	-	-1.15	2.01	1.11
Device: CMP21| SN.: 090279				
Calibrated by	K&Z	K&Z	-	PSA
Calibrated Date	04.11.2009	15.05.2013	-	30.06.2016
Responsivity in µV/(W/m²)	8.67	8.58	-	8.86
Deviation to most recent older responsivity in %	-	-1.04	-	3.29

Table 12. **Calibration history of the field pyrheliometer CHP1_090163**

Device: CHP1 | SN.: 090163			
Calibrated by	K&Z	K&Z	PSA
Calibrated Date	16.11.2009	12.03.2014	30.06.2016
Responsivity in µV/(W/m²)	7.94	7.98	7.95
Deviation to most recent older responsivity in %	-	0.50	-0.37

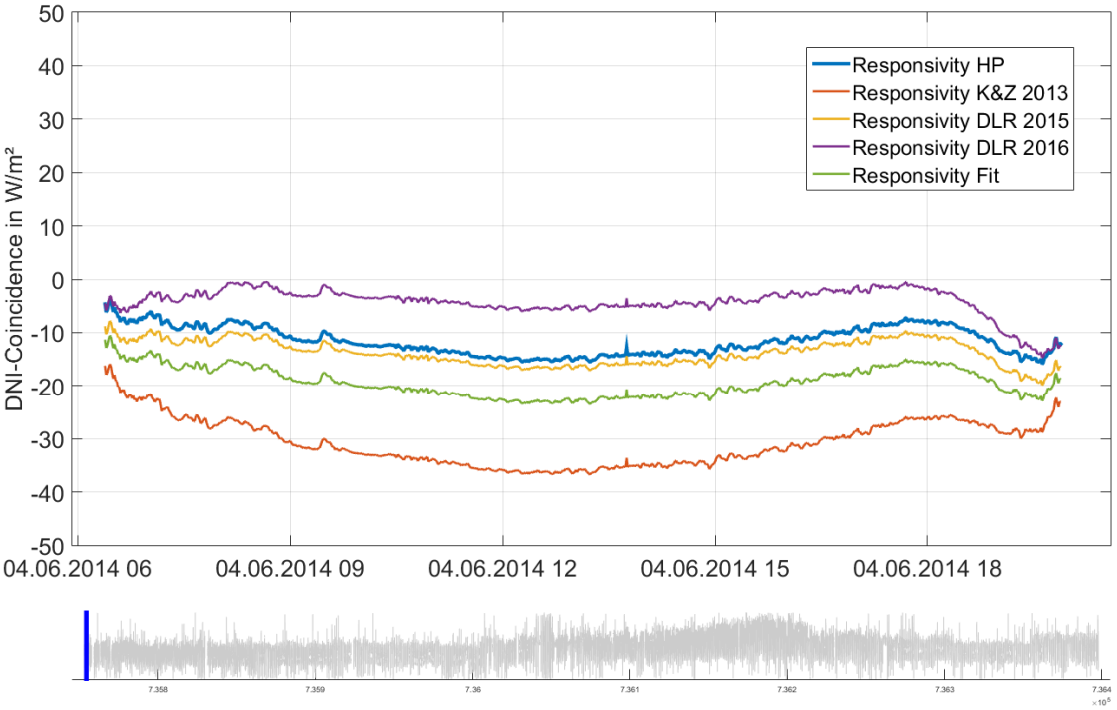
Responsivity HP
Responsivity K&Z 2013
Responsivity DLR 2015
Responsivity DLR 2016
Responsivity Fit
DNI-Coincidence in W/m²
50
40
30
20
10
0
-10
-20
-30
-40
-50
04.06.2014 06
04.06.2014 09
04.06.2014 12
04.06.2014 15
04.06.2014 18

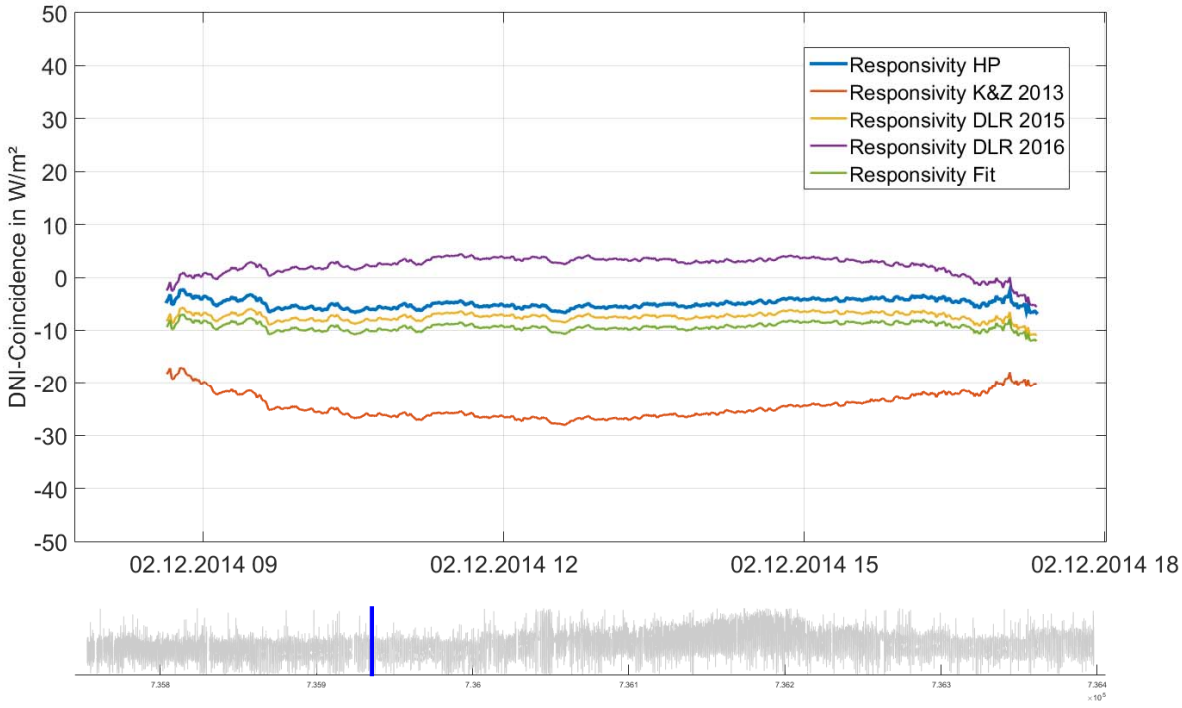
Responsivity HP
Responsivity K&Z 2013
Responsivity DLR 2015
Responsivity DLR 2016
Responsivity Fit
DNI-Coincidence in W/m²
50
40
30
20
10
0
-10
-20
-30
-40
-50
02.12.2014 09
02.12.2014 12
02.12.2014 15
02.12.2014 18
Date Time in dd.mm.yyyy HH

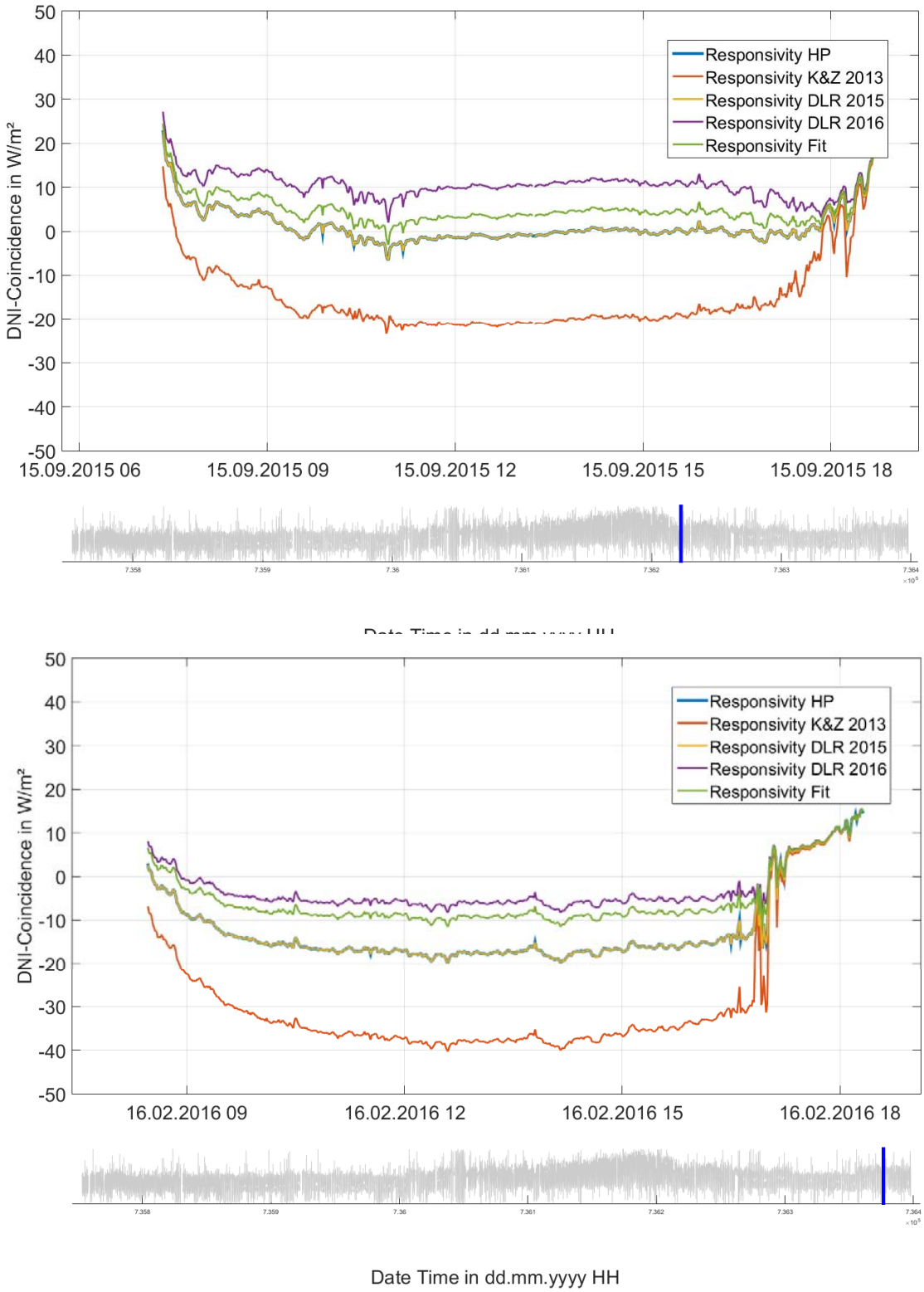

Figure 13. **DNI-coincidence measured at the DLR PSA HP meteorological station with different responsivities for DHI (CMP21_090292) and GHI (CHP1_090163) signal, for four evenly distributed days around the 21 month lasting time period (CC: calibration constant)**

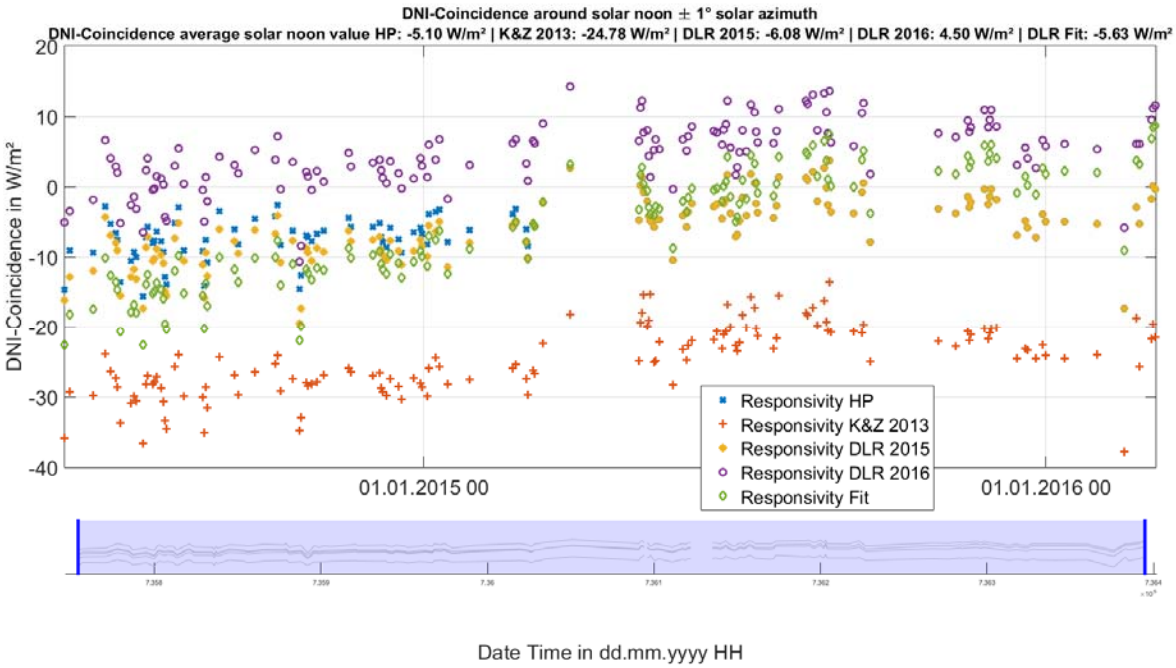

Figure 14. **DNI-Coincidence measured at the DLR PSA HP meteorological station with different responsivities for DHI (CMP21_090292) and GHI (CHP1_090163) signal, average values around solar noon ±1° solar azimuth only clear sky days (CC: calibration constant or responsivity)**

4.4 Results Pyranometer calibration alternating sun-and-shade method

The alternating sun-and-shade method was applied for the DHI reference sensor (CMP22 110288) in the 2015 calibration campaign. On four days of the 2015 campaign, the necessary data were taken.

4.4.1 Obtained valid DNI, DHI and GHI data from reference and test device

The data obtained are illustrated in Figure 15. Figure 15 illustrates also the automated data filtration and averaging. In total 136 measurement phases were obtained. These were distributed over 14 series. Every series starts and ends with a DHI measurement. Some DHI measurements were shared by two series, but never across days. Figure 16 illustrates the generated series. Only the phases marked with a black circle are considered as valid after the filtration process. Data chosen for the further evaluation are highlighted. The calculated Rs values of the series are shown in Figure 17. During a further filtration process some series were rejected:

Rsi values are rejected if deviation to corresponding Rs value ≥ 1%

Rs values are rejected if they consist of less than 3 Rsi values

Rs values are rejected if deviation to R value ≥ 1%

Valid Rs values are marked with a black circle.

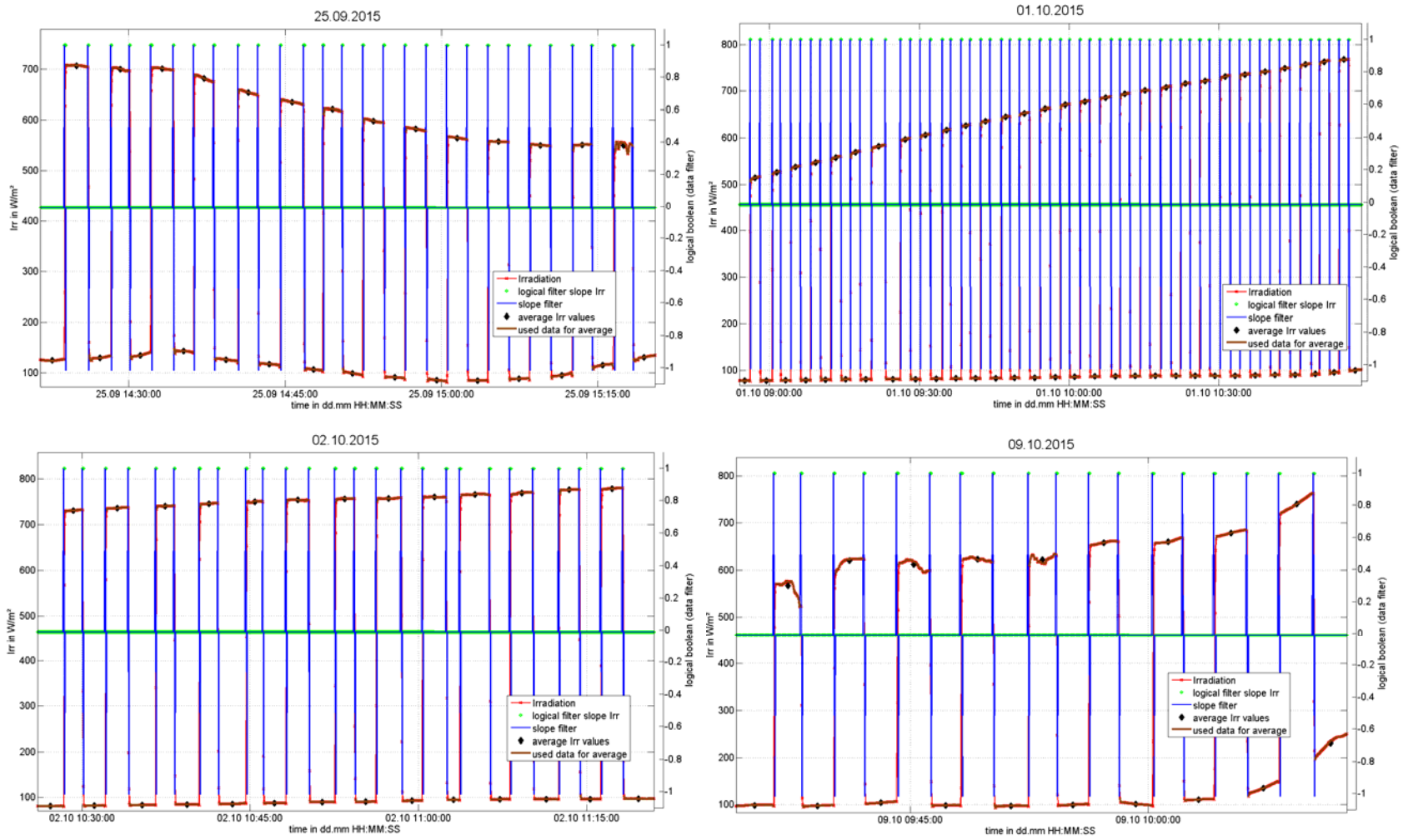

Figure 15. **Data for the alternating sun-and-shade of the four measurement days in 2015. The red lines show the alternating DHI and GHI measurement. The brown highlighted parts of the line show the filtered data. The black diamonds show the average irradiance of that phase.**

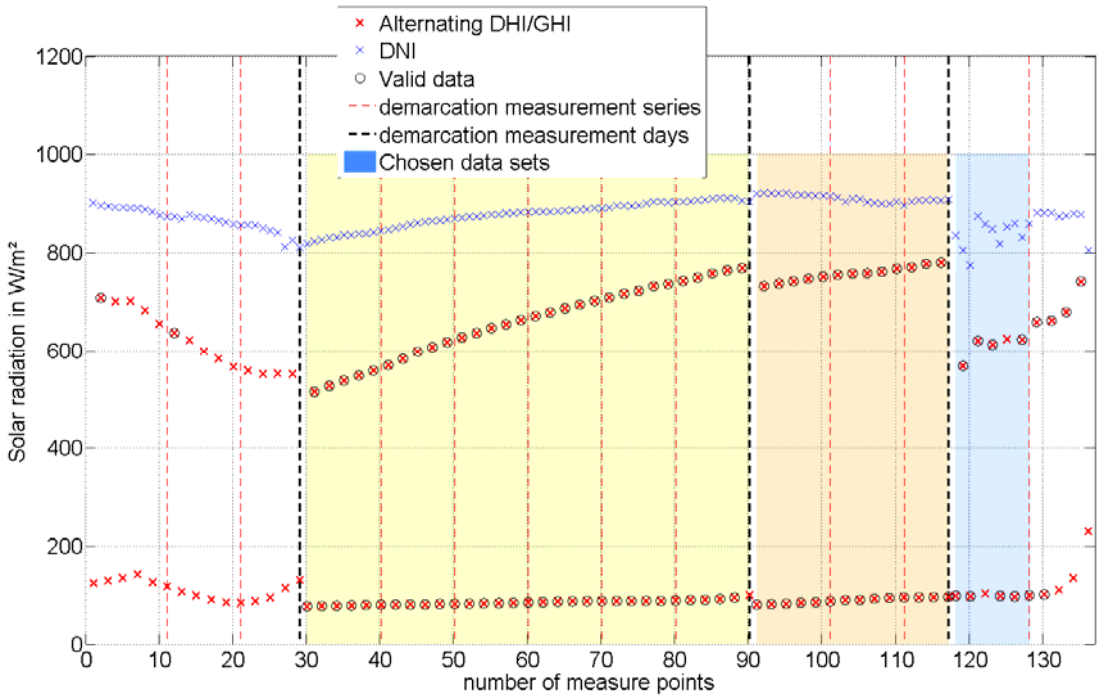

Figure 16. **Filtered and averaged data for alternating sun-and-shade pyranometer calibration method. Only data points with a black circle are valid. The highlighted areas were marked for further evaluation.**

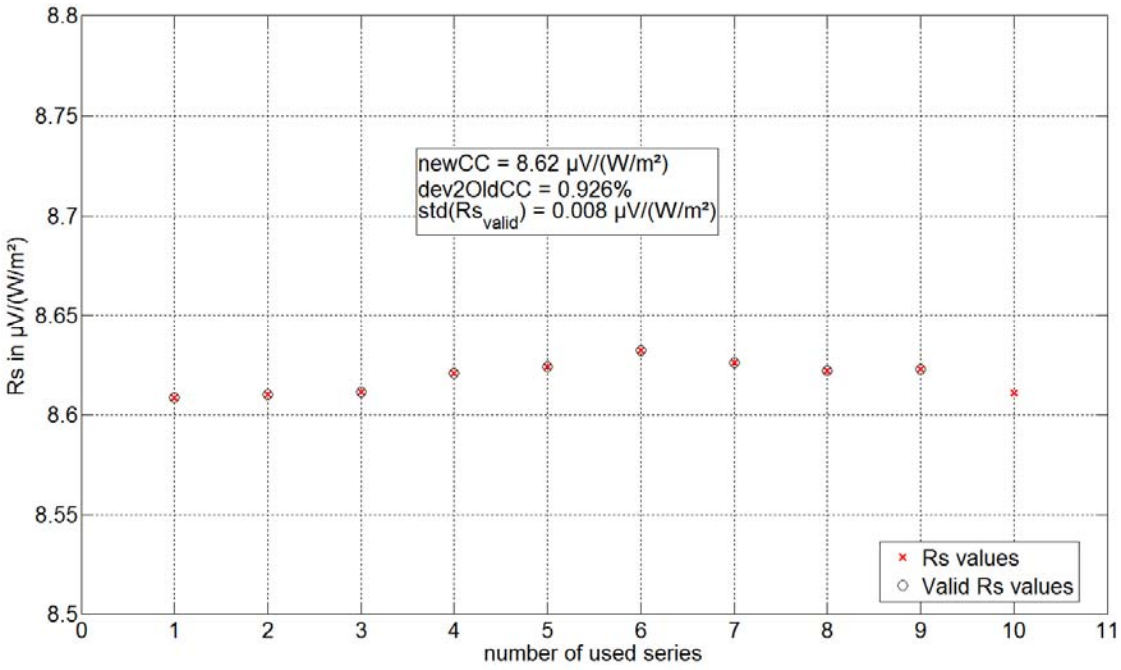

Figure 17. **Calculated responsivities of marked series and new calibration factor for the pyranometer. Only data points with a black circle are valid and used for the new calibration factor.**

4.4.2 Discussion of results for the alternating sun-and-shade method

A new responsivity of 8.62 µV/(W/m²) was calculated. The standard deviation of the used valid Rs values is <0.01 µV/(W/m²).

The test device was originally calibrated by the manufacturer Kipp&Zonen in September 2011. Shortly after the 2015 PSA calibration campaign the test device was send to Kipp&Zonen for a recalibration. All three obtained responsivities are stated in Table 13. The effective operation time of the sensor in between the first two calibrations amounts to about 3 months distributed over 4 years. The PSA field calibration achieved a responsivity about 0.94% higher than the original K&Z responsivity from 2011. The deviation of 0.94% is higher than the expected 1% drift per year of usage. The K&Z calibration taken one month after the PSA field calibration reduces the deviation in responsivity absolutely by half. The deviation between the K&Z and DLR calibration from 2015 lies well within the standard uncertainties of both calibrations.

Table 13. **Evolution of CMP22 | 10288 responsivity in time.**

Calibrated by	K&Z	DLR	K&Z
Calibration Date	12.09.2011	09.10.2015	30.11.2015
Responsivity in µV/(W/m²)	8.54	8.62	8.58
Deviation to most recent older responsivity in %	-	0.94	-0.46

4.5 Influence of cloud filtering on sensor responsivity – filtering with a whole sky imager system

Data filtering using the smallest occurring angular distance between the sun and the clouds is a complicated process. It is time consuming and difficult to accurately estimate if a cloud is closer than 15° away from the sun. For the exclusion of data that is influenced by clouds a whole sky imager (WSI) system was used. The object is to automatically derive the smallest angular distance between the sun and the clouds using the WSI images.

The image processing of the WSI aims to detect cloud positions via image segmentation methods. A four dimensional clear sky library is used (pixel to the zenith (zenith-pixel-angle), the distance of the pixel to the sun (sun-pixel-angle), pressure corrected air mass and Linke turbidity). The images' red to blue ratios (RBR) are compared pixel-wise to the clear sky RBR. If the RBR in the pixel under examination is greater than the RBR of the clear sky library plus a given threshold the pixel is assumed to be cloudy.

Each image pixel of the internal and externally calibrated camera images can be associated with a certain elevation and azimuth angle. With this information, a region around the sun can be projected to the image to check and visualize the required minimum angular distance of the cloud to the sun. The images from the calibration campaign are processed and the minimum angular distance of clouds to the sun and the cloud cover are saved for the further filtering of the irradiance and voltage signals. When the limits are exceeded, timestamps are saved for the subsequent data exclusion during the evaluation.

The left image of Figure 18 shows the acceptance region of 15° around the sun (blue). The distance of the closest detected cloud is represented by the red line. The right image of Figure 18 shows an invalid timestamp which was filtered out automatically during the calibration.

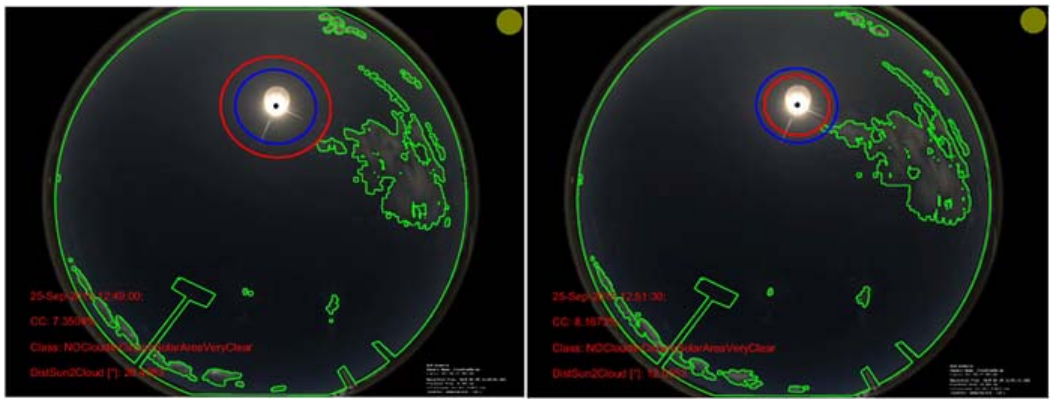

Figure 18. **The blue ring around the sun shows the region within 15° from the sun and the red ring indicates the distance of the closest clouds. Left: Valid conditions; Right: invalid conditions**

The WSI system was tested during the 2015 calibration campaign. Calibrations have been performed once with the WSI based filtering and once without any cloud distance filtering. A third manually filtered data set (using camera videos), is used as a reference. In order to show the importance of the cloud filtering, the case without the WSI based filter uses the complete data set and all other automatic filters, but no manual filtering for the angular cloud distance to the sun. This situation corresponds to a worst case scenario for the quality of the subjective cloud observations of the human observer.

The results of the pyrheliometer calibration remain unchanged for all of the 15 calibrated pyrheliometers. The standard filters according to ISO 9059 are apparently sufficient for the sky conditions faced during the exemplary campaign.

The results for the pyranometer calibration on the other hand change noticeably due to the cloud filtering. The automatic WSI filter detected 98.6% of the cases with clouds 15° or less away from the sun. The standard automatic filters applied for the continuous sun-and-shade method do not exclude data points even if a high DHI or low DNI was measured.

The effect of the filtering is also clearly visible in the results of the calibration of the nine field pyranometers that were calibrated in this example. This holds for the resulting responsivities and also for the standard deviations. Figure 19 shows the responsivities R of the test pyranometers at a solar zenith angle of 45° obtained with the three different cloud filters. Without cloud filtering high relative deviations of R to the reference of up to 0.42 % occur. The relative deviation between the result for the automatic WSI based filter and the reference is small (<0.01%).

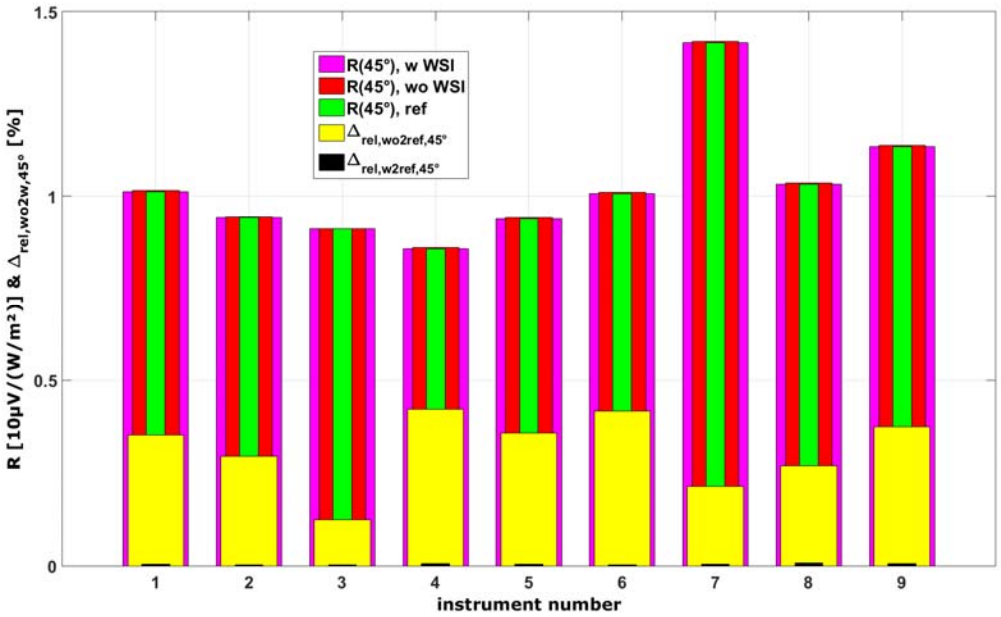

Figure 19. **Comparison of pyranometer responsivities derived for a solar zenith angle of 45° with the reference filter (green), with WSI based filtering (magenta) and without WSI based filtering (red). The relative deviations of the results without cloud distance filtering to the reference are shown in yellow. The relative deviations of the results with automatic WSI filtering to the reference are shown in black.**

5 Conclusion

The partners Ciemat and DLR improved the joint calibration facility for pyrheliometers and pyranometers at PSA and conducted three individual calibration campaigns.

- First campaign period 19.06.2014 to 30.06.2014
- Second campaign period 23.09.2015 to 09.10.2015
- Third campaign period 20.06.2016 to 30.06.2016

CNRS supported the 2016 campaign during a two week stay of CNRS scientist at the third PSA calibration campaign.
Each campaign included a pyrheliometer calibration according to the ISO standard 9059 and a continuous sun-and-shade method pyranometer calibration according to ISO standard 9846. A total of 80 new responsivities were derived from the calibration data:

- 18 x Kipp&Zonen CHP1 pyrheliometer
- 7 x Kipp&Zonen CH1 pyrheliometer
- 3 x Hukseflux DR02/3 pyrheliometer
- 23 x Eppley Nip pyrheliometer
- 3 x Kipp&Zonen CMP22 pyranometer
- 18 x Kipp&Zonen CM/CMP21 pyranometer
- 7 x Kipp&Zonen CM/CMP11 pyranometer
- 1 x Hukseflux SR12-T1-05 pyranometer

For the pyrheliometers the absolute average deviation between the newly acquired responsivity compared to the most recent older responsivity was around 0.6%. At PSA repeatedly calibrated pyrheliometer showed deviations between the campaigns significantly lower than the average deviation.

Pyranometer field calibration yielded systematically in average 0.6% higher responsivity than the manufacturer laboratory calibration. Varies worldwide distributed metrological stations in operation by Ciemat and DLR show also systematically a negative DNI-coincidence, which might be partly explained by a systematically to low manufacturer responsivity for pyranometers. However this has to be investigated more closely.

A detailed examination of the solar azimuth and zenith angle dependency on the pyranometer responsivity was conducted during the 2016 campaign. In the solar elevation angle interval that is interesting for solar energy production, a fluctuation around 0.5 percentage points of the responsivity between forenoon and afternoon was observed. For high zenith angles (>60°) fluctuations rise considerable. It seems reasonable to implement individual generated solar angle dependent variable responsivities for pyranometer.

A possible faulty manufacturer calibration was detected for four pyranometers (around 2%).

During the 2015 campaign an additional alternating sun-and-shade method pyranometer calibration was conducted on the CMP22 DHI reference sensor. A manufacturer calibration conducted immediately afterwards showed a deviation around 0.4% between the PSA outdoor calibration and the manufacturer laboratory calibration and confirmed the calibration result from PSA within the uncertainties of the two calibrations.

A new WSI (whole sky imager) based data filtering method was developed and demonstrated. The effect of the cloud distance filtering has shown to be negligible for pyrheliometer calibration, but it is crucial for pyranometer calibration during partially cloudy conditions. For the 2015 calibration campaign with complicated cloud conditions deviations of the determined pyranometer responsivity of up to 0.42 % were found if no cloud distance filter was used. Future versions of the ISO calibration standards should further stress the importance of the cloud filtering. Also stricter outlier rejection might be considered for pyranometer calibration as the 5 % limit was found to be too tolerant.

References

[Sfera2 D11_2, 2015] Sfera 2 deliverable task report 11.2, Report on established joint calibration facility for pyrheliometers at PSA to be operated as ACCESS facility, B. Nouri et al., Tabernas (Spain) 2016

[ISO, 1990] International Organization for Standardization, ISO 9059:1990 Solar energy - Calibration of field pyrheliometers by comparison to a reference pyrheliometer, international standard, Geneva (Switzerland) 1990

[ISO, 1993] International Organization for Standardization, ISO 9846:1993 Solar energy - Calibration of a pyranometer using a pyrheliometer, international standard, Geneva (Switzerland) 1993

[ISO, 1992] International Organization for Standardization, ISO 9847:1992 Solar energy - Calibration of a pyranometer using a reference pyranometer, international standard, Geneva (Switzerland) 1992

[PMOD, 2009] Physikalisch-Meteorologisches Observatorium Davos, PMO6 Operating Manual (Version 2.1), Tech. Rep., Davos (Switzerland)

[PfiffnerEmail, 2016] Email contact between Daniel Pfiffner from PMOD and Bijan Nouri from DLR, Davos (Switzerland), 05.10.2016

List of Figures

FIGURE 1. TOP) OVERVIEW OF METAS CALIBRATION SETUP (1: PYRANOMETER TEST BENCH; 2: PYRHELIOMETERS TEST BENCH; 3: BLACK PHOTON TRACKER WITH DHI REFERENCE; 4: CLOUD CAMERA); BOTTOM LEFT) DETAIL VIEW OF BLACK PHOTON TRACKER; BOTTOM LEFT CENTRE) DETAIL VIEW OF PYRHELIOMETER TEST BENCH; BOTTOM RIGHT CENTRE) TWO ABSOLUTE CAVITY REFERENCE PYRHELIOMETERS LOCATED AT PYRHELIOMETER TEST BENCHFRONT CABINET; BOTTOM RIGHT) METAS WIND MAST. 5
FIGURE 2. ORDER OF EVENTS ABSOLUTE CAVITY DNI MEASUREMENT (BASED ON [PMOD, 2009]) 9
FIGURE 3. AMBIENT CONDITIONS DURING 2014 CALIBRATION CAMPAIGN (DAY 1: 19.06.2014, DAY 2: 20.06.2014, DAY 3: 25.06.2014, DAY 4: 26.06.2014, DAY5: 27.06.2014 AND DAY 6: 30.06.2014) 11
FIGURE 4. AMBIENT CONDITIONS DURING 2015 CALIBRATION CAMPAIGN (DAY 1: 23.09.2015, DAY 2: 24.09.2015, DAY 3: 25.09.2015, DAY 4: 28.09.2015, DAY5: 30.09.2015, DAY 6: 01.10.2015, DAY 7: 02.10.2015, DAY 8: 06.10.2015 AND DAY 9: 09.10.2015) 12
FIGURE 5. AMBIENT CONDITIONS DURING 2016 CALIBRATION CAMPAIGN (DAY 1: 20.06.2016, DAY 2: 21.06.2016, DAY 3: 22.06.2016, DAY 4: 23.06.2016, DAY5: 24.06.2016, DAY 6: 27.06.2016, DAY 7: 29.06.2016 AND DAY 8: 30.06.2016) 13
FIGURE 6. 2014 PYRHELIOMETER CAMPAIGN; TOP) VALID AND INVALID REFERENCE DATA; BOTTOM) MARKER FOR ACTIVE FILTER OF THE INVALID DATA 15
FIGURE 7. 2015 PYRHELIOMETER CAMPAIGN; TOP) VALID AND INVALID REFERENCE DATA; BOTTOM) MARKER FOR ACTIVE FILTER OF THE INVALID DATA 16
FIGURE 8. 2016 PYRHELIOMETER CAMPAIGN; TOP) VALID AND INVALID REFERENCE DATA; BOTTOM) MARKER FOR ACTIVE FILTER OF THE INVALID DATA 17

FIGURE 9. 2014 PYRANOMETER CAMPAIGN; TOP) VALID AND INVALID REFERENCE DATA; BOTTOM) MARKER FOR ACTIVE FILTER OF THE INVALID DATA 23
FIGURE 10. 2015 PYRANOMETER CAMPAIGN; TOP) VALID AND INVALID REFERENCE DATA; BOTTOM) MARKER FOR ACTIVE FILTER OF THE INVALID DATA 24
FIGURE 11. 2016 PYRANOMETER CAMPAIGN; TOP) VALID AND INVALID REFERENCE DATA; BOTTOM) MARKER FOR ACTIVE FILTER OF THE INVALID DATA 25
FIGURE 12. **TYPICAL DNI-COINCIDENCE OF CLEAR SKY DAY MEASURED AT THE DLR PSA HP METEOROLOGICAL STATION** 28
FIGURE 13. **DNI-COINCIDENCE MEASURED AT THE DLR PSA HP METEOROLOGICAL STATION WITH DIFFERENT RESPONSIVITIES FOR DHI (CMP21_090292) AND GHI (CHP1_090163) SIGNAL, FOR FOUR EVENLY DISTRIBUTED DAYS AROUND THE 21 MONTH LASTING TIME PERIOD (CC: CALIBRATION CONSTANT)** 36
FIGURE 14. **DNI-COINCIDENCE MEASURED AT THE DLR PSA HP METEOROLOGICAL STATION WITH DIFFERENT RESPONSIVITIES FOR DHI (CMP21_090292) AND GHI (CHP1_090163) SIGNAL, AVERAGE VALUES AROUND SOLAR NOON ±1° SOLAR AZIMUTH ONLY CLEAR SKY DAYS (CC: CALIBRATION CONSTANT OR RESPONSIVITY)** 37
FIGURE 15. **DATA FOR THE ALTERNATING SUN-AND-SHADE OF THE FOUR MEASUREMENT DAYS IN 2015. THE RED LINES SHOW THE ALTERNATING DHI AND GHI MEASUREMENT. THE BROWN HIGHLIGHTED PARTS OF THE LINE SHOW THE FILTERED DATA. THE BLACK DIAMONDS SHOW THE AVERAGE IRRADIANCE OF THAT PHASE.** 39
FIGURE 16. **FILTERED AND AVERAGED DATA FOR ALTERNATING SUN-AND-SHADE PYRANOMETER CALIBRATION METHOD. ONLY DATA POINTS WITH A BLACK CIRCLE ARE VALID. THE HIGHLIGHTED AREAS WERE MARKED FOR FURTHER EVALUATION.** 40
FIGURE 17. **CALCULATED RESPONSIVITIES OF MARKED SERIES AND NEW CALIBRATION FACTOR FOR THE PYRANOMETER. ONLY DATA POINTS WITH A BLACK CIRCLE ARE VALID AND USED FOR THE NEW CALIBRATION FACTOR.** 40
FIGURE 18. **THE BLUE RING AROUND THE SUN SHOWS THE REGION WITHIN 15° FROM THE SUN AND THE RED RING INDICATES THE DISTANCE OF THE CLOSEST CLOUDS. LEFT: VALID CONDITIONS; RIGHT: INVALID CONDITIONS** 42
FIGURE 19. **COMPARISON OF PYRANOMETER RESPONSIVITIES DERIVED FOR A SOLAR ZENITH ANGLE OF 45° WITH THE REFERENCE FILTER (GREEN), WITH WSI BASED FILTERING (MAGENTA) AND WITHOUT WSI BASED FILTERING (RED). THE RELATIVE DEVIATIONS OF THE RESULTS WITHOUT CLOUD DISTANCE FILTERING TO THE REFERENCE ARE SHOWN IN YELLOW. THE RELATIVE DEVIATIONS OF THE RESULTS WITH AUTOMATIC WSI FILTERING TO THE REFERENCE ARE SHOWN IN BLACK.** 43

List of Tables

TABLE 1. **AT CALIBRATION CAMPAIGNS USED REFERENCE SENSORS** 6
TABLE 2. **ENTIRE LIST OF CARRIED OUT MEASUREMENT DAYS WITH COMMENTS OF DATA STATUS** 10
TABLE 3. **LIST ON CALIBRATION CAMPAIGNS PARTICIPATING FIELD PYRHELIOMETER WITH RESULTS FOR NEW RESPONSIVITY** 18
TABLE 4. **AVERAGE DEVIATION AND ABSOLUTE AVERAGE DEVIATION TO MOST RECENT OLDER RESPONSIVITIES (ONLY THE SENSORS FIRST APPEARANCE AT A PSA CALIBRATION CAMPAIGN; WITHOUT OUTLIER SENSORS) AND AVERAGE RSD OF NEW RESPONSIVITY (PYRHELIOMETER)** 20
TABLE 5. **RESPONSIVITIES AND DEVIATION TO MOST RECENT OLDER RESPONSIVITY FOR REPEATEDLY CALIBRATED SENSORS (PYRHELIOMETER)** 21
TABLE 6. **LIST ON CALIBRATION CAMPAIGNS PARTICIPATING FIELD PYRANOMETER WITH RESULTS FOR NEW RESPONSIVITIES** 26

TABLE 7. **ABSOLUTE AVERAGE DEVIATION TO MOST RECENT OLDER RESPONSIVITIES (ONLY THE SENSORS FIRST APPEARANCE AT A PSA CALIBRATION CAMPAIGN; WITHOUT OUTLIER SENSORS) AND AVERAGE RSD OF NEW RESPONSIVITY (PYRANOMETER)** 28
TABLE 8. **RESPONSIVITIES AND DEVIATION TO MOST RECENT OLDER RESPONSIVITY FOR REPEATEDLY CALIBRATED SENSORS (PYRANOMETER)** 29
TABLE 9. **PYRANOMETER SOLAR AZIMUTH AND ZENITH ANGLE DEPENDENT RESPONSIVITIES IN μV/(W/M²) AND DEVIATION IN % (ONLY 2016 CAMPAIGN)** 30
TABLE 10. **PYRANOMETER MIN ZENITH ANGLE RESPONSIVITIES COMPARED WITH MOST RECENT MANUFACTURER RESPONSIVITIES IN μV/(W/M²) AND DEVIATION IN % (ONLY 2016 CAMPAIGN)** 32
TABLE 11. **CALIBRATION HISTORY OF THE FIELD PYRANOMETERS CMP21_090292, CMP21_090280, CMP21_090281 AND CMP21_090279** 34
TABLE 12. **CALIBRATION HISTORY OF THE FIELD PYRHELIOMETER CHP1_090163** 34
TABLE 13. **EVOLUTION OF CMP22 | 10288 RESPONSIVITY IN TIME.** 41

List of abbreviations and definitions

WRR	World Radiometric Reference
PSA	Plataforma Solar de Almería
ACR	Absolute Cavity Radiometer
DAS	Data Acquisition System
WSI	Whole Sky Imager
METAS	Meteorological Station for Solar Technologies
ASSM	Alternating Sun-and-Shade Method
CoSSM	Continuous Sun-and-Shade Method
DNI	Direct Normal Irradiance
GHI	Global Horizontal Irradiance
DHI	Diffuse Horizontal Irradiance
rsd	Relative standard deviation
std	Standard deviation